



Engineering the electronic and optical properties of a-Se through Ge alloying for photodetection



Kaitlin Hellier

Radiological Instrumentation Laboratory

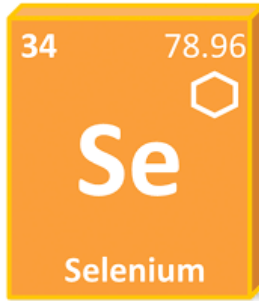
Electrical and Computer Engineering

ril.soe.ucsc.edu

UC SANTA CRUZ

 Baskin
Engineering

Amorphous Selenium



www.hruimetal.com

Selenium is part of the **chalcogen group** (Group VI) in the periodic table, along with oxygen, sulfur, tellurium, and polonium.

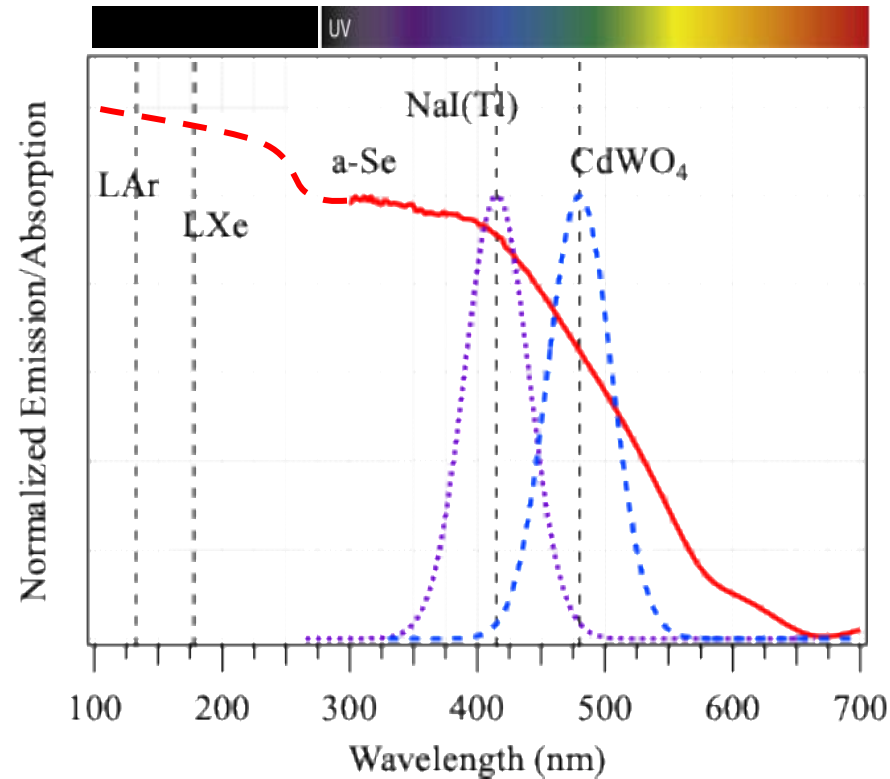
Amorphous selenium is widely used in **X-ray detectors**.

Benefits:

- Large area, low cost, maturity
- Good absorption properties for relatively low energy
- Low dark current ($E_g = 2.2\text{eV}$)
- **Potential for gain (avalanche)**
- High spatial resolution (direct detector)

A-Se as Indirect Conversion: Pushing the Limit of Sensitivity

Matching Sensitivity Spectrum of Photodetector with Emission of Scintillator



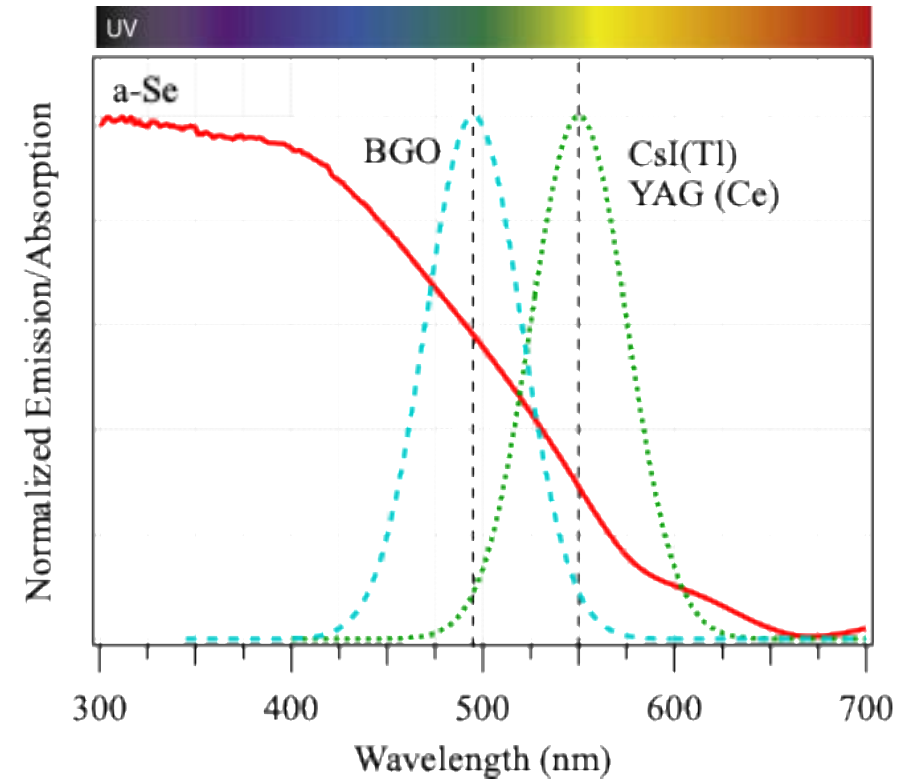
a-Se is an excellent absorber for VUV-UV-Blue emitters like liquid Ar & Xe, NaI, undoped CsI where other diodes fail

— Leiga, A., *J. Opt. Soc. Am.* (1968) v 58, 11, p 1441

A-Se as Indirect Conversion: Pushing the Limit of Sensitivity

Matching Sensitivity Spectrum of Photodetector with Emission of Scintillator

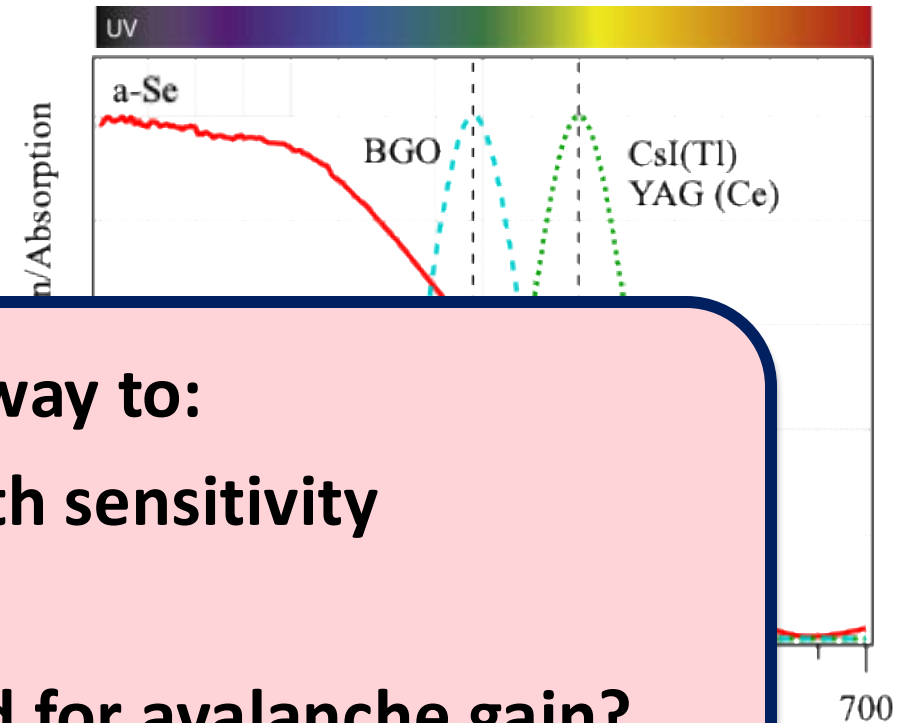
But has low absorption – and low efficiency – for high-yield, higher resolution long-wavelength emitters



A-Se as Indirect Conversion: Pushing the Limit of Sensitivity

Matching Sensitivity Spectrum of Photodetector with Emission of Scintillator

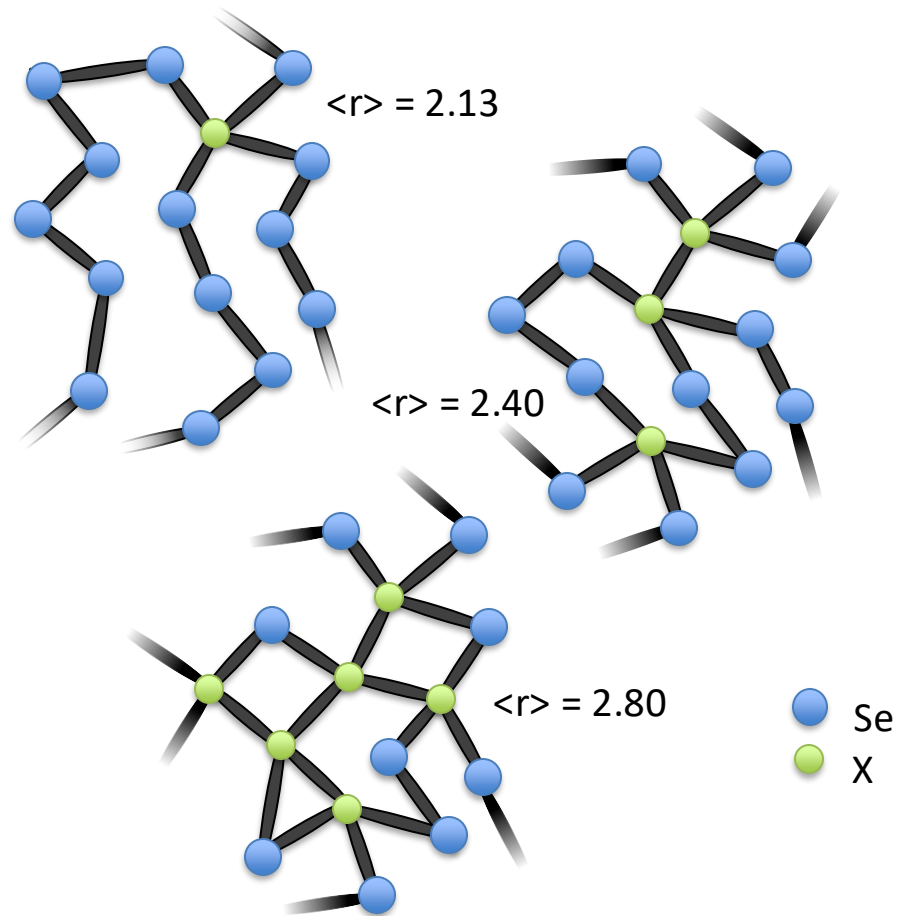
But has low absorption – and low efficiency – for high-yield, higher



Can we find a way to:

- 1) Achieve long-wavelength sensitivity
- 2) Increase transport
- 3) Lower the field required for avalanche gain?

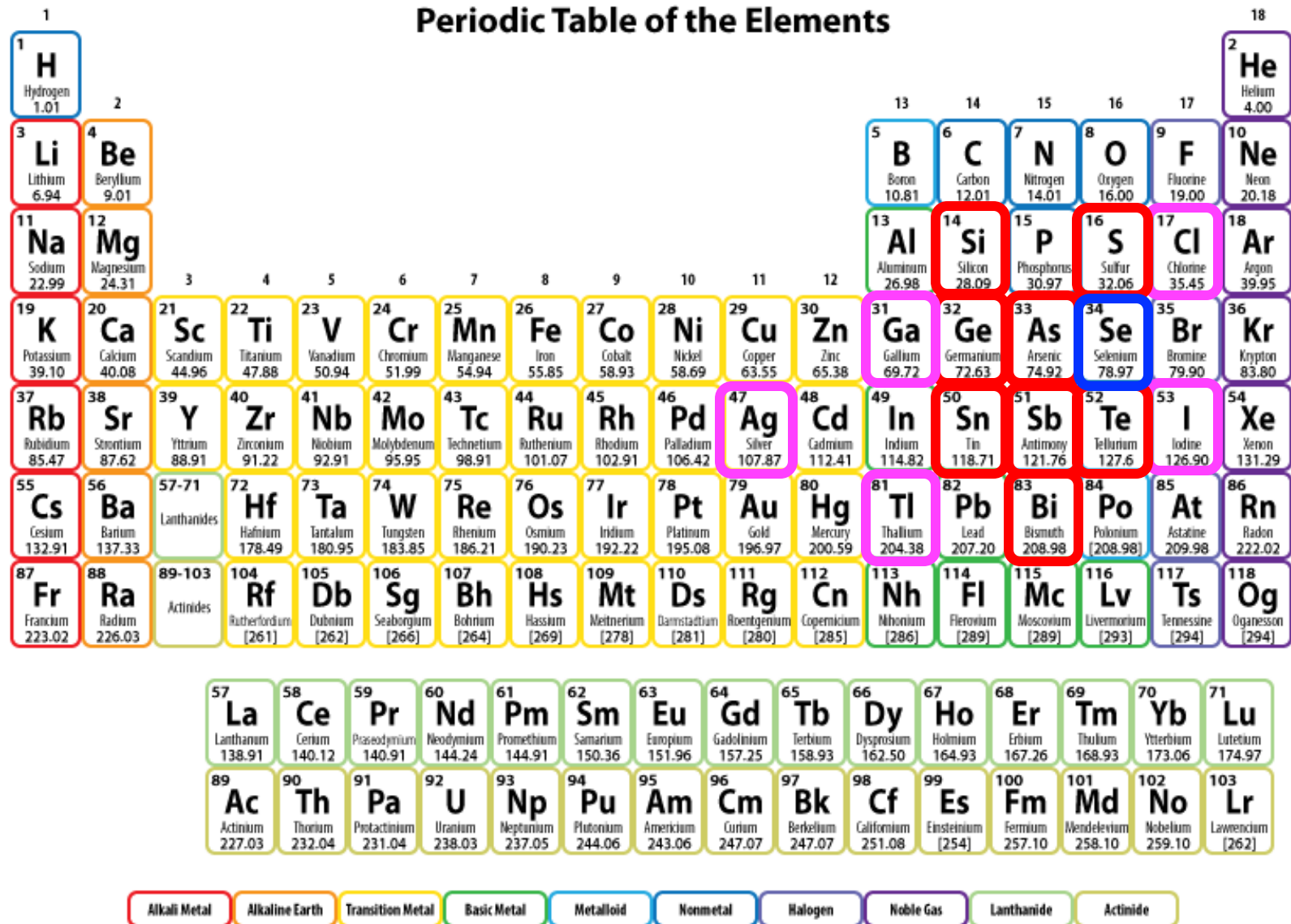
Doping and Alloying with Group IV, V, & VI elements



Can change properties such as:

- Band gap
- Leakage currents
- Carrier transport
- Sensitivity
- Structure & coordination
- Crystallization
- Stability

Doping and Alloying with Group IV, V, & VI elements



Doping and Alloying with Group IV, V, & VI elements

Arsenic

- Doped at 0.1 – 0.5 %
- Stabilizes, preventing crystallization
- Introduces deep hole trap states, lowering carrier lifetime

Chlorine

- 10-40 ppm
- Mitigates deep hole traps from As
- Improves carrier lifetimes, with minimal effect on mobilities

Periodic Table of the Elements

1 H Hydrogen 1.01																	2 He Helium 4.00
3 Li Lithium 6.94	4 Be Beryllium 9.01											5 B Boron 10.81	6 C Carbon 12.01	7 N Nitrogen 14.01	8 O Oxygen 16.00	9 F Fluorine 19.00	10 Ne Neon 20.18
11 Na Sodium 22.99	12 Mg Magnesium 24.31											13 Al Aluminum 26.98	14 Si Silicon 28.09	15 P Phosphorus 30.97	16 S Sulfur 32.06	17 Cl Chlorine 35.45	18 Ar Argon 39.95
19 K Potassium 39.10	20 Ca Calcium 40.08	21 Sc Scandium 44.96	22 Ti Titanium 47.88	23 V Vanadium 50.94	24 Cr Chromium 51.99	25 Mn Manganese 54.94	26 Fe Iron 55.85	27 Co Cobalt 58.93	28 Ni Nickel 58.69	29 Cu Copper 63.55	30 Zn Zinc 65.38	31 Ga Gallium 69.72	32 Ge Germanium 72.63	33 As Arsenic 74.92	34 Se Selenium 78.97	35 Br Bromine 79.90	36 Kr Krypton 83.80
37 Rb Rubidium 85.47	38 Sr Strontium 87.62	39 Y Yttrium 88.91	40 Zr Zirconium 91.22	41 Nb Niobium 92.91	42 Mo Molybdenum 95.95	43 Tc Technetium 98.91	44 Ru Ruthenium 101.07	45 Rh Rhodium 102.91	46 Pd Palladium 106.42	47 Ag Silver 107.87	48 Cd Cadmium 112.41	49 In Indium 114.82	50 Sn Tin 118.71	51 Sb Antimony 121.76	52 Te Tellurium 127.6	53 I Iodine 126.90	54 Xe Xenon 131.29
55 Cs Cesium 132.91	56 Ba Barium 137.33	57-71 Lanthanides	72 Hf Hafnium 178.49	73 Ta Tantalum 180.95	74 W Tungsten 183.85	75 Re Rhenium 186.21	76 Os Osmium 190.23	77 Ir Iridium 192.22	78 Pt Platinum 195.08	79 Au Gold 196.97	80 Hg Mercury 200.59	81 Tl Thallium 204.38	82 Pb Lead 207.20	83 Bi Bismuth 208.98	84 Po Polonium (208.98)	85 At Astatine 209.98	86 Rn Radon 222.02
87 Fr Francium 223.02	88 Ra Radium 226.03	89-103 Actinides	104 Rf Rutherfordium [261]	105 Db Dubnium [262]	106 Sg Seaborgium [266]	107 Bh Bohrium [264]	108 Hs Hassium [269]	109 Mt Meitnerium [278]	110 Ds Darmstadtium [281]	111 Rg Roentgenium [280]	112 Cn Copernicium [285]	113 Nh Nihonium [286]	114 Fl Flerovium [289]	115 Mc Moscovium [289]	116 Lv Livermorium [293]	117 Ts Tennessine [294]	118 Og Oganesson [294]

57 La Lanthanum 138.91	58 Ce Cerium 140.12	59 Pr Praseodymium 140.91	60 Nd Neodymium 144.24	61 Pm Promethium 144.91	62 Sm Samarium 150.36	63 Eu Europium 151.96	64 Gd Gadolinium 157.25	65 Tb Terbium 158.93	66 Dy Dysprosium 162.50	67 Ho Holmium 164.93	68 Er Erbium 167.26	69 Tm Thulium 168.93	70 Yb Ytterbium 173.06	71 Lu Lutetium 174.97
89 Ac Actinium 227.03	90 Th Thorium 232.04	91 Pa Protactinium 231.04	92 U Uranium 238.03	93 Np Neptunium 237.05	94 Pu Plutonium 244.06	95 Am Americium 243.06	96 Cm Curium 247.07	97 Bk Berkelium 247.07	98 Cf Californium 251.08	99 Es Einsteinium [254]	100 Fm Fermium 257.10	101 Md Mendelevium 258.10	102 No Nobelium 259.10	103 Lr Lawrencium [262]

Alkali Metal	Alkaline Earth	Transition Metal	Basic Metal	Metalloid	Nonmetal	Halogen	Noble Gas	Lanthanide	Actinide
--------------	----------------	------------------	-------------	-----------	----------	---------	-----------	------------	----------

Kasap et. al, *JMS Mat. in Elec.* (2000), v 11, 3, p 179

Kasap et. al, *Semiconductors*, (2003) v 37, 7, p 789

Doping and Alloying with Group IV, V, & VI elements

Periodic Table of the Elements

Tellurium

- Increasing Te decreases E_g
- Induces traps, lowering μ and τ
- Increases conductivity
- Increases crystallization temperature

Germanium

- Ge may lower E_g , however studies differ
- Lowers μ_e , then increases
- Increases thermal stability
- Properties are very content dependent

57 La Lanthanum 138.91	58 Ce Cerium 140.12	59 Pr Praseodymium 140.91	60 Nd Neodymium 144.24	61 Pm Promethium 144.91	62 Sm Samarium 150.36	63 Eu Europium 151.96	64 Gd Gadolinium 157.25	65 Tb Terbium 158.93	66 Dy Dysprosium 162.50	67 Ho Holmium 164.93	68 Er Erbium 167.26	69 Tm Thulium 168.93	70 Yb Ytterbium 173.06	71 Lu Lutetium 174.97
89 Ac Actinium 227.03	90 Th Thorium 232.04	91 Pa Protactinium 231.04	92 U Uranium 238.03	93 Np Neptunium 237.05	94 Pu Plutonium 244.06	95 Am Americium 243.06	96 Cm Curium 247.07	97 Bk Berkelium 247.07	98 Cf Californium 251.08	99 Es Einsteinium [254]	100 Fm Fermium 257.10	101 Md Mendelevium 258.10	102 No Nobelium 259.10	103 Lr Lawrencium [262]

Alkali Metal	Alkaline Earth	Transition Metal	Basic Metal	Metalloid	Nonmetal	Halogen	Noble Gas	Lanthanide	Actinide
--------------	----------------	------------------	-------------	-----------	----------	---------	-----------	------------	----------

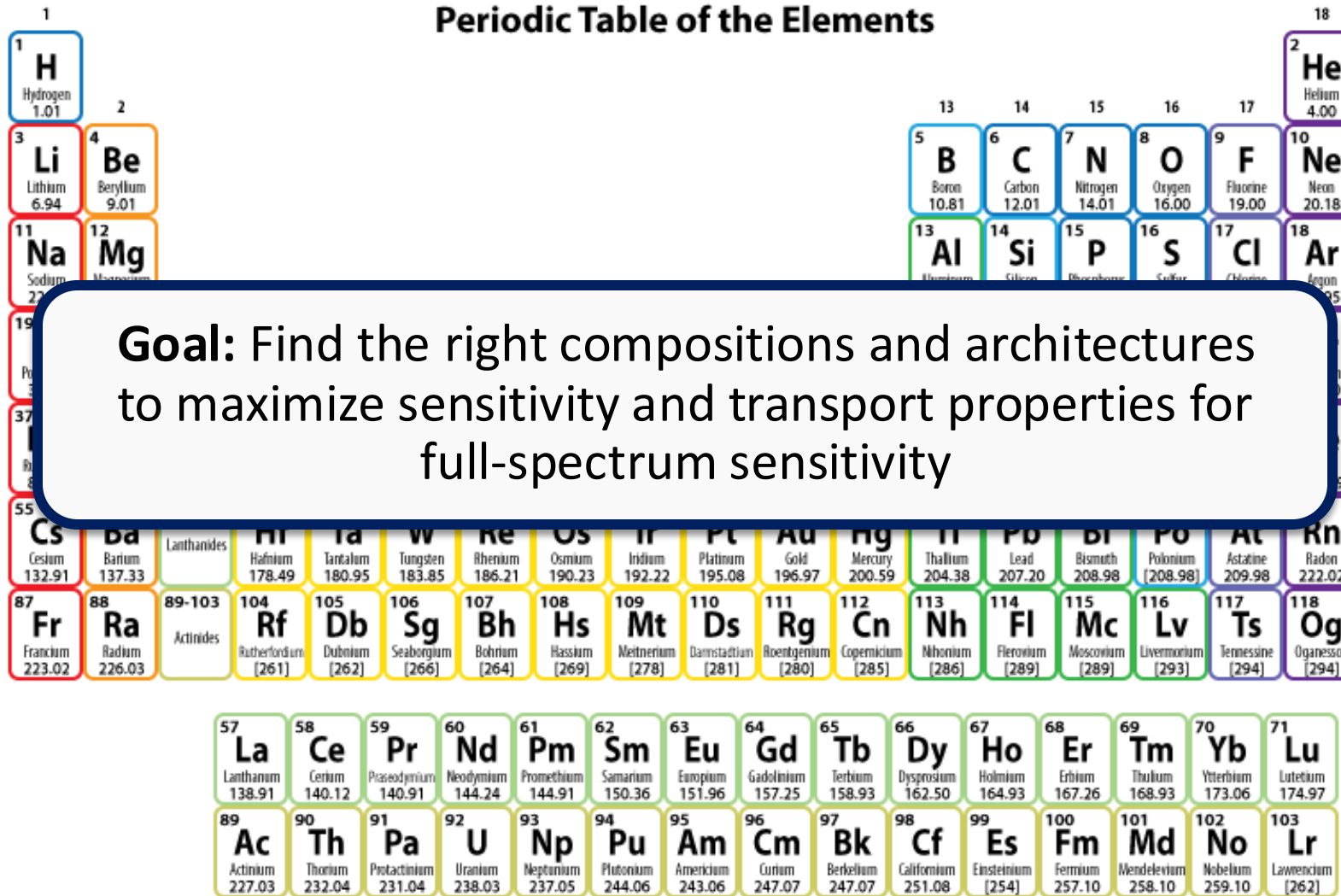
Hellier et. al, *ACS AEM* (2023), v 5, 5, p 2678

Nang, et al., *Jpn. JAP* (1976), v 15, 5, p 849

Kim & Shirafuji, *Jap. JAP* (1978), v 17, 10, p 1789

Doping and Alloying with Group IV, V, & VI elements

Periodic Table of the Elements



Tellurium

- Increasing Te decreases E_g
- Induces traps, lowering μ and τ
- Increases conductivity
- Increases crystallization temperature

Germanium

- Ge may lower E_g , however studies differ
- Lowers μ_e , then increases
- Increases thermal stability
- Properties are very content dependent

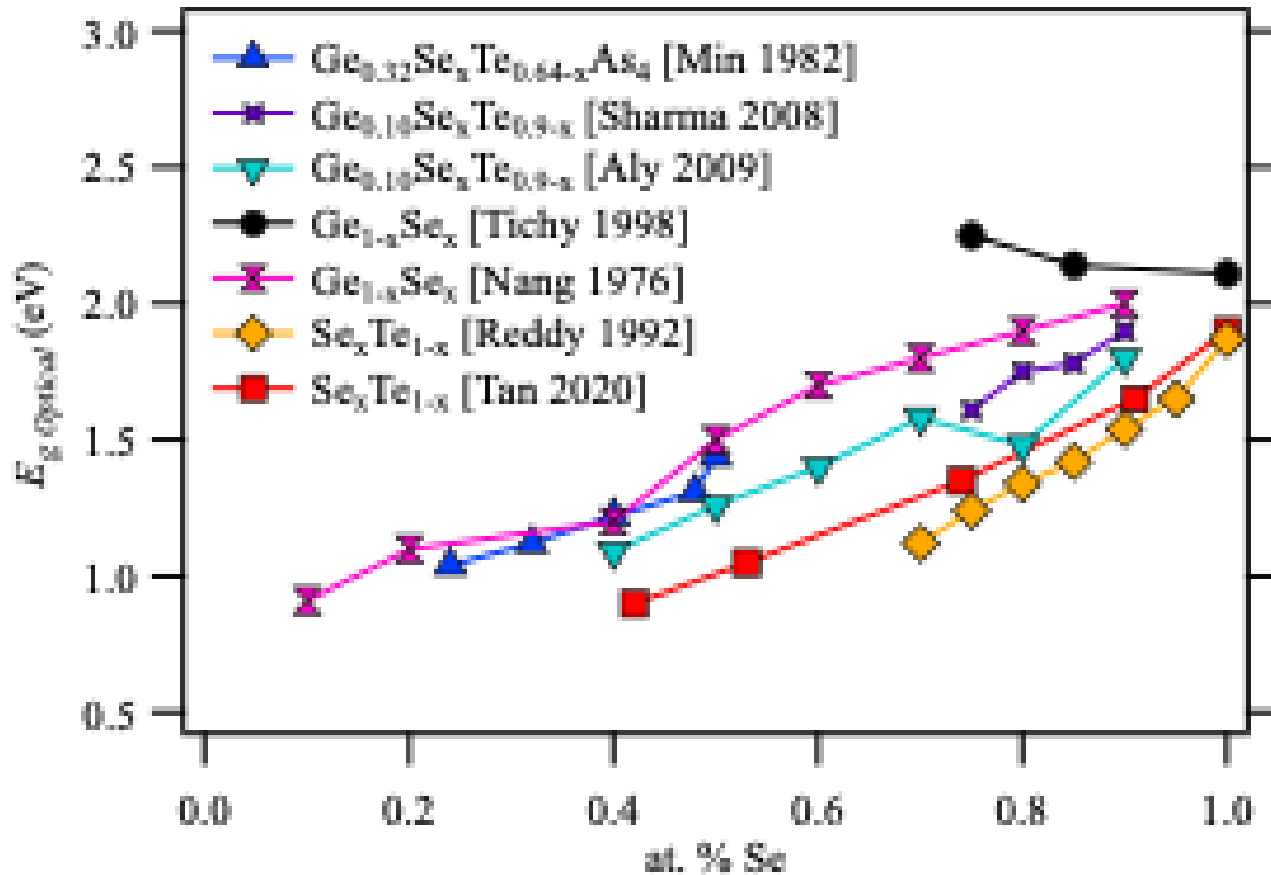
Hellier et. al, *ACS AEM* (2023), v 5, 5, p 2678

Nang, et al., *Jpn. JAP* (1976), v 15, 5, p 849

Kim & Shirafuji, *Jap. JAP* (1978), v 17, 10, p 1789



Doping and Alloying with Group IV, V, & VI elements



- Se-Te previously investigated for photodetection, solar cells, memory applications
- Ge-Se & Ge-Se-Te primarily investigated for switching devices, memory
 - Literature reaches differing conclusions on optical and electronic properties, **leaving questions waiting to be answered**

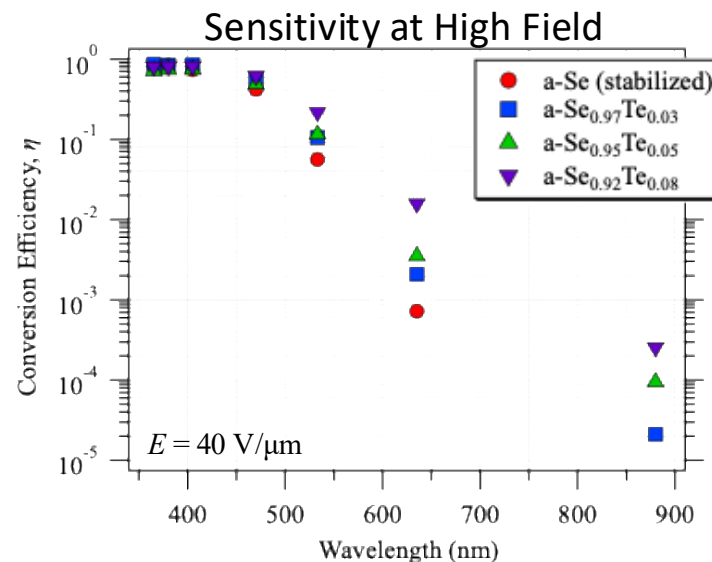
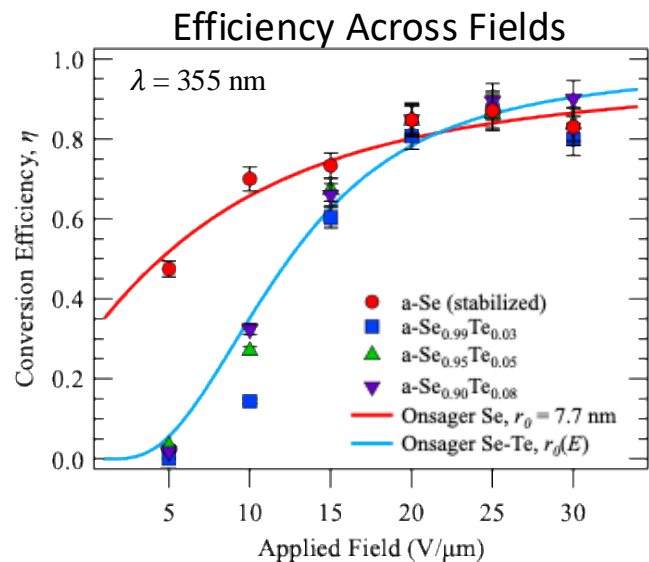
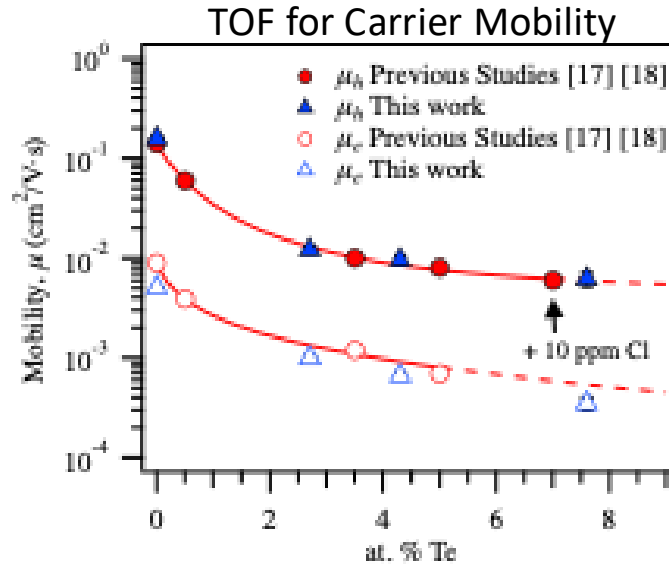
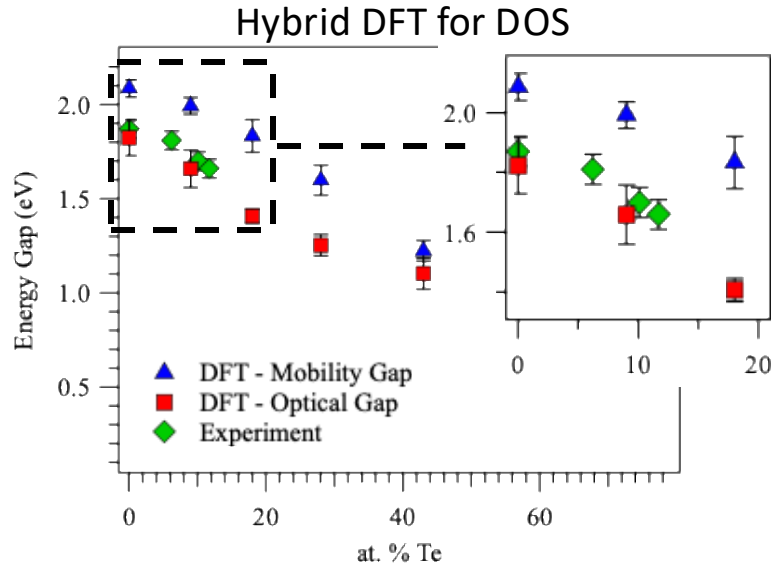
Sample	E_g (eV)	x	E_g^{opt} (eV)
a-Se	2.11 ± 0.01	0.1	2.0
a- $\text{Ge}_{15}\text{Se}_{85}$	2.14 ± 0.01	0.2	1.9
a- $\text{Ge}_{25}\text{Se}_{75}$	2.25 ± 0.01	0.3	1.8
		0.33	—
		0.4	1.7
		0.5	1.5
		0.6	1.2
		0.7	—
		0.8	1.1
		0.9	0.91

↖ L. Tichy, et al., *J. Non-Cryst. Sol.* (1998), v 240, 1, p 177

T. T. Nang, et al., *Jpn. J. Appl. Phys.* (1976), v 15, 5, p. 849



Alloying a-Se with Te: Previous Studies



→ Predict band gap and trends with reasonable accuracy

→ Measure carrier transit time to accurately evaluate mobilities

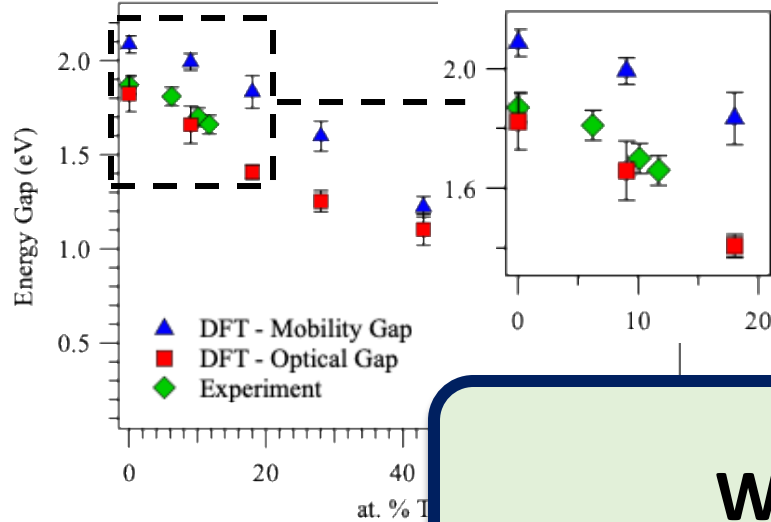
→ Evaluate and model η at high fields to understand transport

→ Detect increased sensitivity to long wavelengths

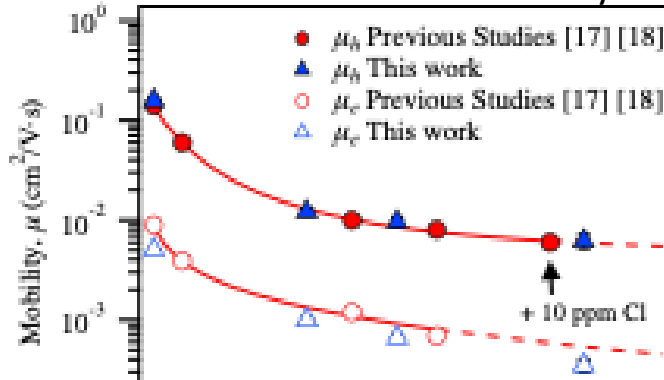
Hellier et. al, *ACS AEM* (2023), v 5, 5, p 2678

Alloying a-Se with Te: Previous Studies

Hybrid DFT for DOS



TOF for Carrier Mobility



→ Predict band gap and trends with reasonable accuracy

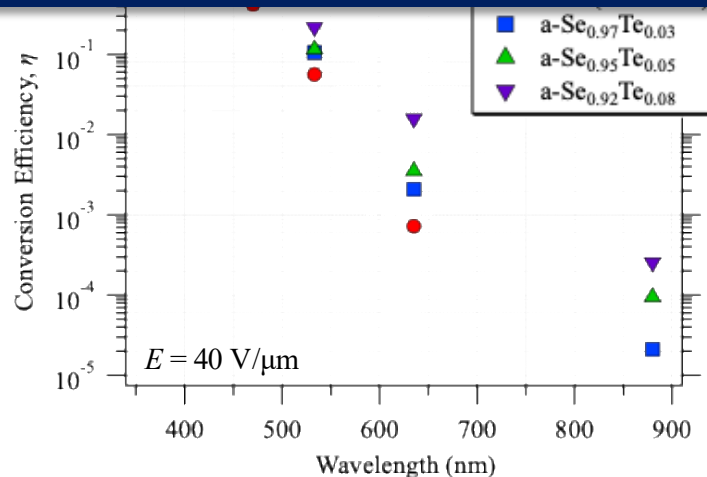
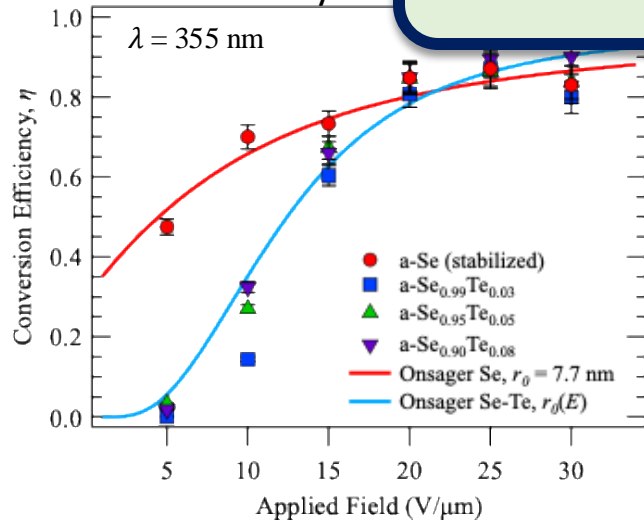
→ Measure carrier transit time to accurately evaluate mobilities

What do we expect from Ge-Se?

→ Evaluate and model η at high fields to understand transport

→ Detect increased sensitivity to long wavelengths

Efficiency Act



Hellier et. al, *ACS AEM* (2023), v 5, 5, p 2678

Alloying a-Se with Ge: Charge Transport

Charge transport with increasing Ge concentration

G. I. Kim, J. Shirafuji, and Y. Inuishi,
 "Transport of Photoexcited Carriers in
 Evaporated $\text{Ge}_x\text{Se}_{1-x}$ Glass Films," *Jpn. J.
 Appl. Phys.*, vol. 20, no. 8, p. 1377, Aug.
 1981

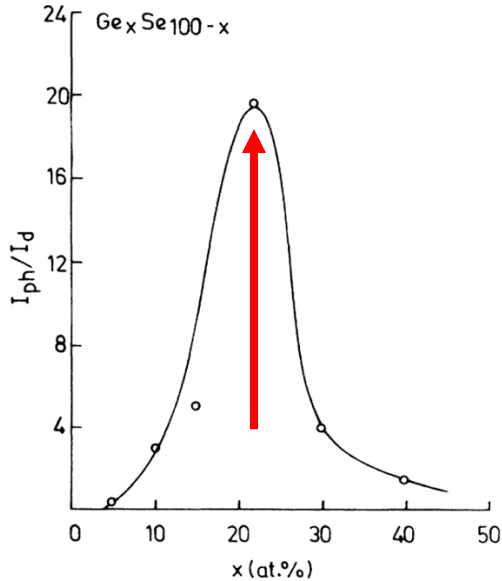
	Scher-Montroll plot	Conventional method	Thickness
(Electron)			
$\text{Ge}_{0.2}\text{Se}_{0.8}$	$2.3 \times 10^{-4} \text{ cm}^2/\text{V}\cdot\text{s}$	$3.1 \times 10^{-4} \text{ cm}^2/\text{V}\cdot\text{s}$	4.5 μm
$\text{Ge}_{0.35}\text{Se}_{0.65}$	1×10^{-3}	1.4×10^{-3}	5.0
(Hole)			
$\text{Ge}_{0.3}\text{Se}_{0.7}$	7.4×10^{-5}	1.0×10^{-4}	5.0
$\text{Ge}_{0.4}\text{Se}_{0.6}$	1.7×10^{-4}	2.1×10^{-4}	5.0

Increasing electron mobility with minimal effect on hole mobility with low Ge concentration

	Holes		Electrons	
	μ_h ($\text{cm}^2/\text{V}\cdot\text{sec}$)	ϵ_h (eV)	μ_e ($\text{cm}^2/\text{V}\cdot\text{sec}$)	ϵ_e (eV)
Se^{9-15}	$1.3 \sim 2 \times 10^{-1}$	0.23~0.28	$6 \sim 7 \times 10^{-3}$	0.26~0.33
$\text{Ge}_{0.03}\text{Se}_{0.97}^{20}$	same as Se		7×10^{-5}	0.51
$\text{Ge}_{0.15}\text{Se}_{0.85}$	8.5×10^{-2}		1.7×10^{-1}	
$\text{Ge}_{0.20}\text{Se}_{0.80}$	3.8×10^{-2}	0.42	1.0×10^{-1}	0.28
$\text{Ge}_{0.40}\text{Se}_{0.60}$	1.6×10^{-2}		7.4×10^{-1}	

G. I. Kim and J. Shirafuji, "Time of Flight
 Measurement of Carrier Mobility in $\text{Ge}_x\text{Se}_{1-x}$
 Glasses," *Jpn. J. Appl. Phys.*, vol. 17, no. 10, p.
 1789, Oct. 1978

Alloying a-Se with Ge: Photoconduction

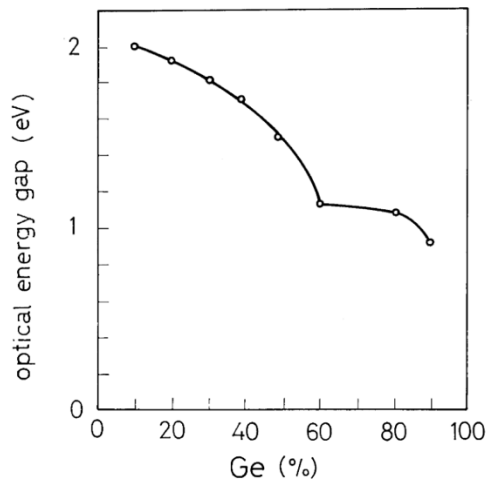


Optimizing photoconductivity as a function of Ge concentration

A. Kumar, "Steady-state and transient photoconductivity in amorphous thin films of Ge_xSe_{100-x} ," *Phys. Rev. B*, vol. 38, no. 18, pp. 13432–13435, 1988

TABLE I. Electrical parameters in amorphous thin films of Ge_xSe_{100-x} at 300 K.

Composition x	σ_d ($\Omega^{-1}cm^{-1}$)	ΔE (eV)	σ_0 ($\Omega^{-1}cm^{-1}$)	σ_{ph} ($\Omega^{-1}cm^{-1}$)	I_{ph}/I_d	ΔE_{ph} (eV)	τ_d (sec)
5	1.2×10^{-7}	0.43	2.8	3.8×10^{-8}	0.4	0.41	107
10	5.0×10^{-10}	0.67	6.9×10^1	1.5×10^{-9}	3.0	0.63	77
15	9.2×10^{-10}	0.71	5.6×10^2	4.4×10^{-9}	5.0	0.59	65
22	1.4×10^{-8}	0.90	1.3×10^7	2.7×10^{-7}	19.7	0.32	54
30	7.5×10^{-10}	0.75	2.2×10^3	3.4×10^{-9}	4.0	0.59	79
40	6.6×10^{-10}	0.50	2.1×10^{-1}	1.0×10^{-9}	1.5	0.47	95

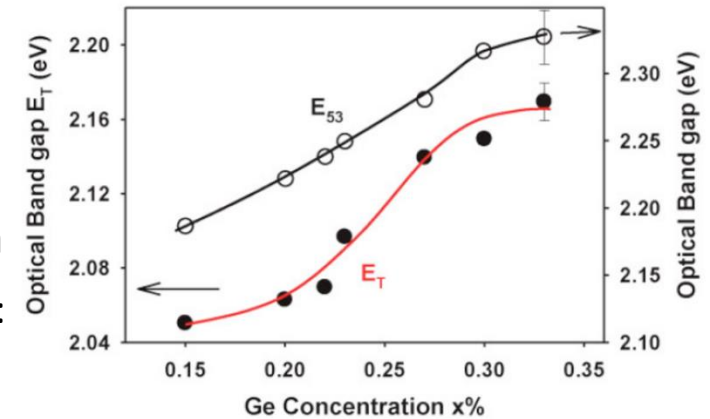


Decreasing Bandgap with Ge concentration

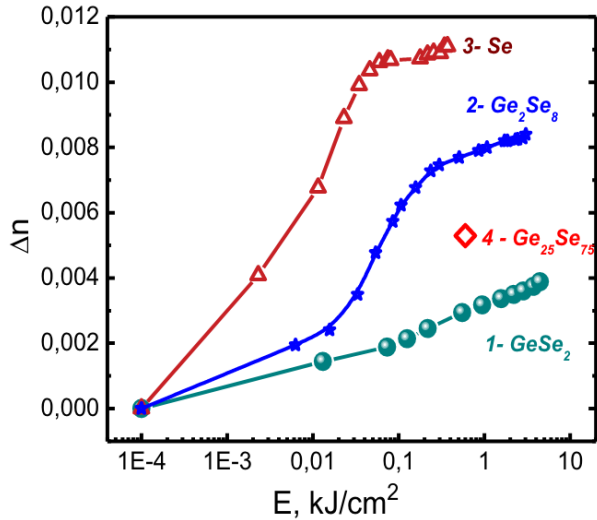
T. T. Nang, M. Okuda, T. Matsushita, S. Yokota, and A. Suzuki, "Electrical and Optical Properties of Ge_xSe_{1-x} Amorphous Thin Films," *Jpn. J. Appl. Phys.*, vol. 15, no. 5, p. 849, May 1976

Increasing Bandgap with Ge concentration

A. Mishchenko, "Amorphous Selenium (a-Se) and its Compounds: Photo-induced Metastability and Application in a Novel Gamma Camera," 2016, Accessed: Nov. 19, 2024.



Alloying a-Se with Ge: Photo-induced Effects

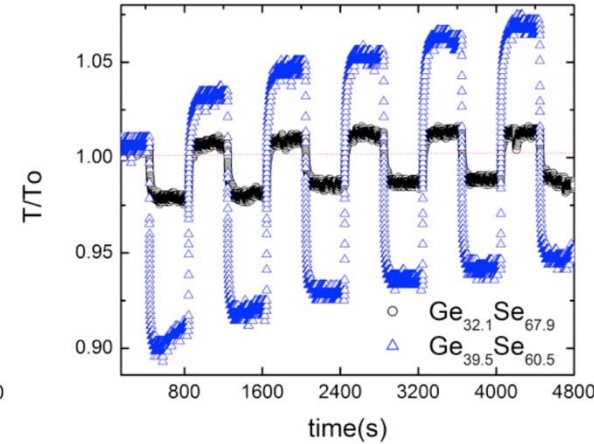
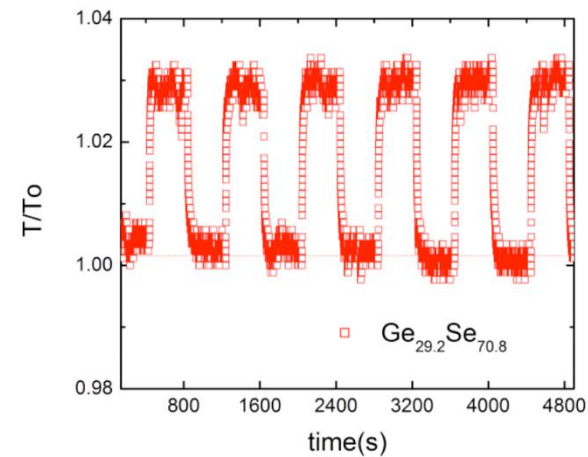


Holographic Recording → Observation of RT Birefringence

M. Reinfelde, M. Mitkova, T. Nichol, Z. G. Ivanova, and J. Teteris, "PHOTOINDUCED MASS TRANSPORT IN Ge-SE AMORPHOUS FILMS," *Chalcogenide Letters*, vol. 15, no. 1, p. 35, 2018.

Photodarkening & Photobleaching for Ge > 30%

A. Mishchenko, J. Berashevich, K. Wolf, D. A. Tenne, A. Reznik, and M. Mitkova, "Dynamic variations of the light-induced effects in a- $\text{Ge}_x\text{Se}_{100-x}$ films: experiment and simulation," *Opt. Mater. Express*, *OME*, vol. 5, no. 2, pp. 295–306, Feb. 2015



Photodarkening After Illumination

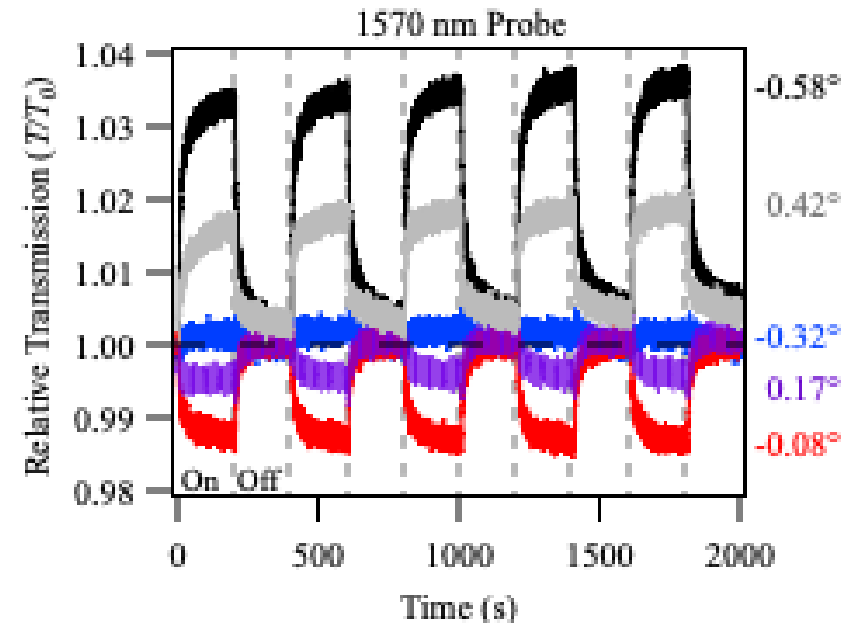
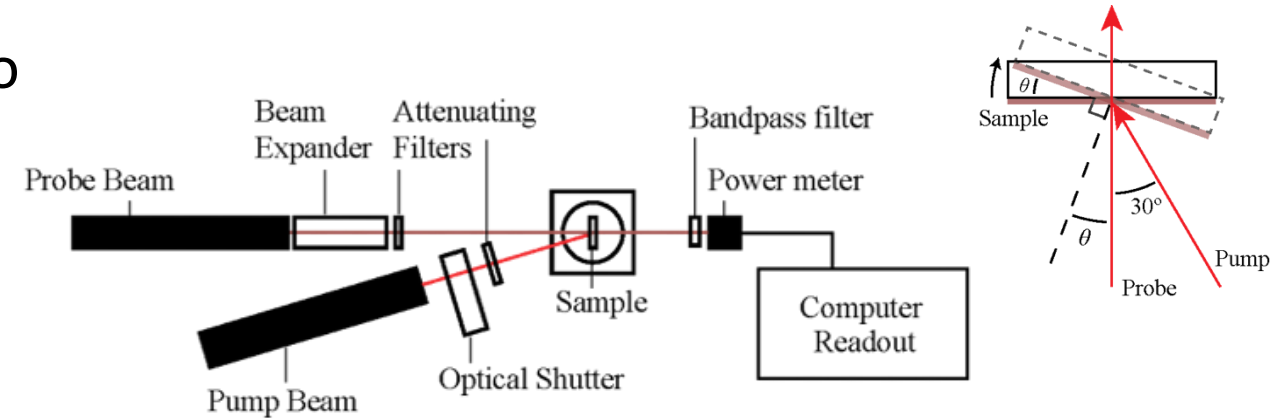
L. Tichy, H. Ticha, P. Nagels, and R. Callaerts, "Photoinduced optical changes in amorphous Se and Ge–Se films," *Journal of Non-Crystalline Solids*, vol. 240, no. 1, pp. 177–181, Oct. 1998

Sample	E_g (v)	E_g (120)
a-Se	2.11 ± 0.01	1.97 ± 0.01
a- $\text{Ge}_{15}\text{Se}_{85}$	2.14 ± 0.01	1.99 ± 0.01
a- $\text{Ge}_{25}\text{Se}_{75}$	2.25 ± 0.01	2.14 ± 0.01

Photo-induced Effects in a-Se

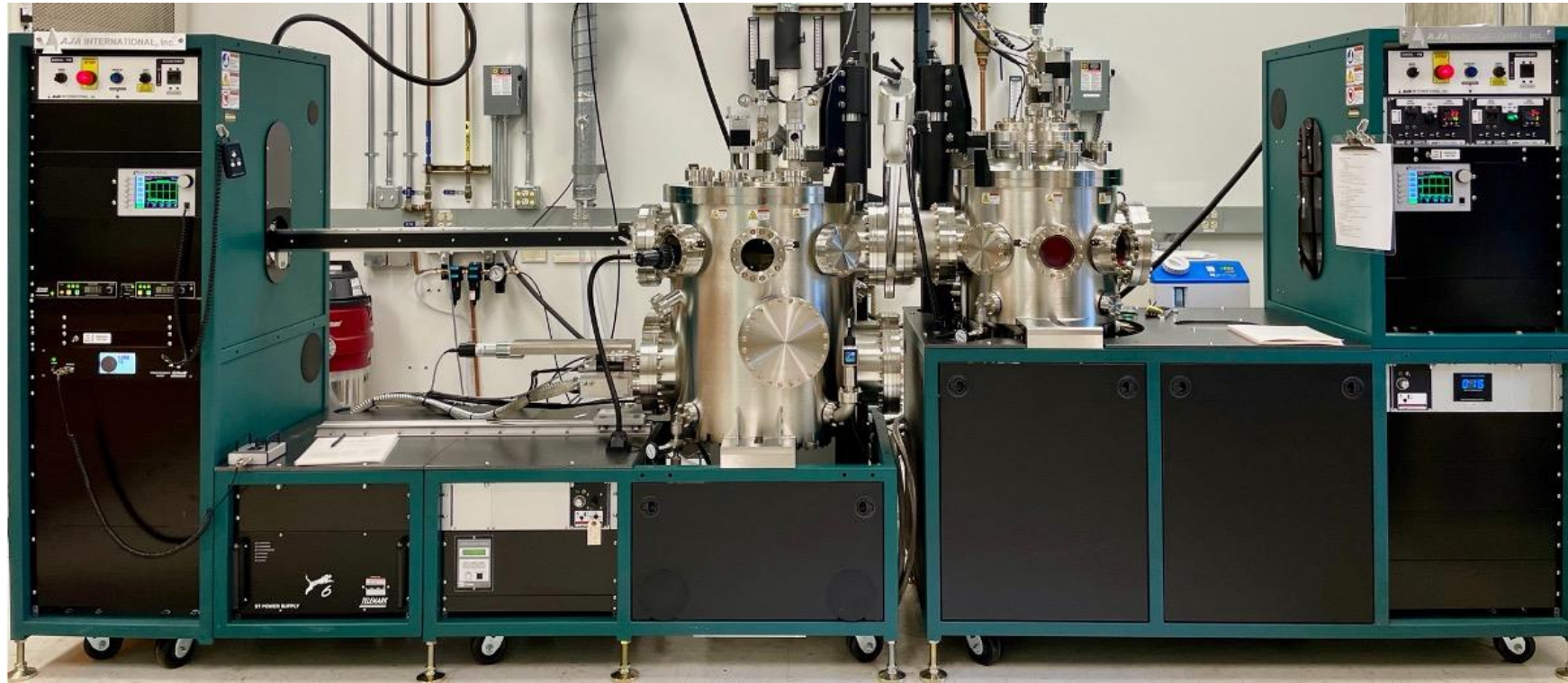
- a-Se undergoes darkening when exposed to near bandgap wavelengths
 - Increases trap states due to metastable structural changes during exposure
- Probing with SWIR light leads to angle dependence in transmission
 - *Increase* in transmission for angles off normal

Additional Goal: exploit for detection with knowledge of propagation direction of incident light → Alloying may increase effects!



Hellier et. al, *IEEE TED* (2024), v 71, 8, p 4808

RIL Fabrication Facilities



- Custom-built, dedicated selenium thermal evaporator and e-beam deposition systems
- One of the few U.S. research facilities capable of uniform, large area (>4"Ø) a-Se detector fabrication



Prof. Shiva Abbaszadeh
Associate Professor



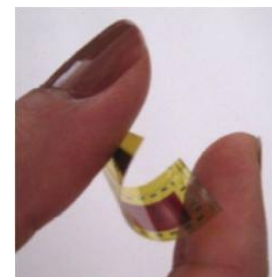
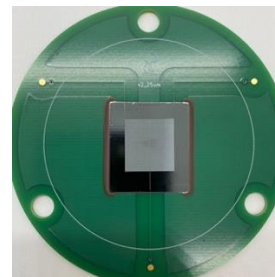
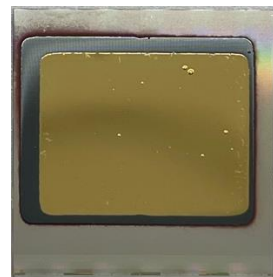
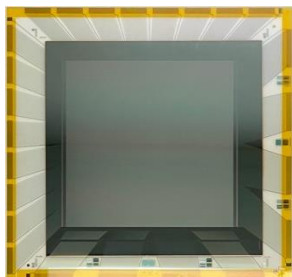
Dr. Kaitlin Hellier
Postdoctoral Scholar



Hamid Mirzanezhad
PhD student

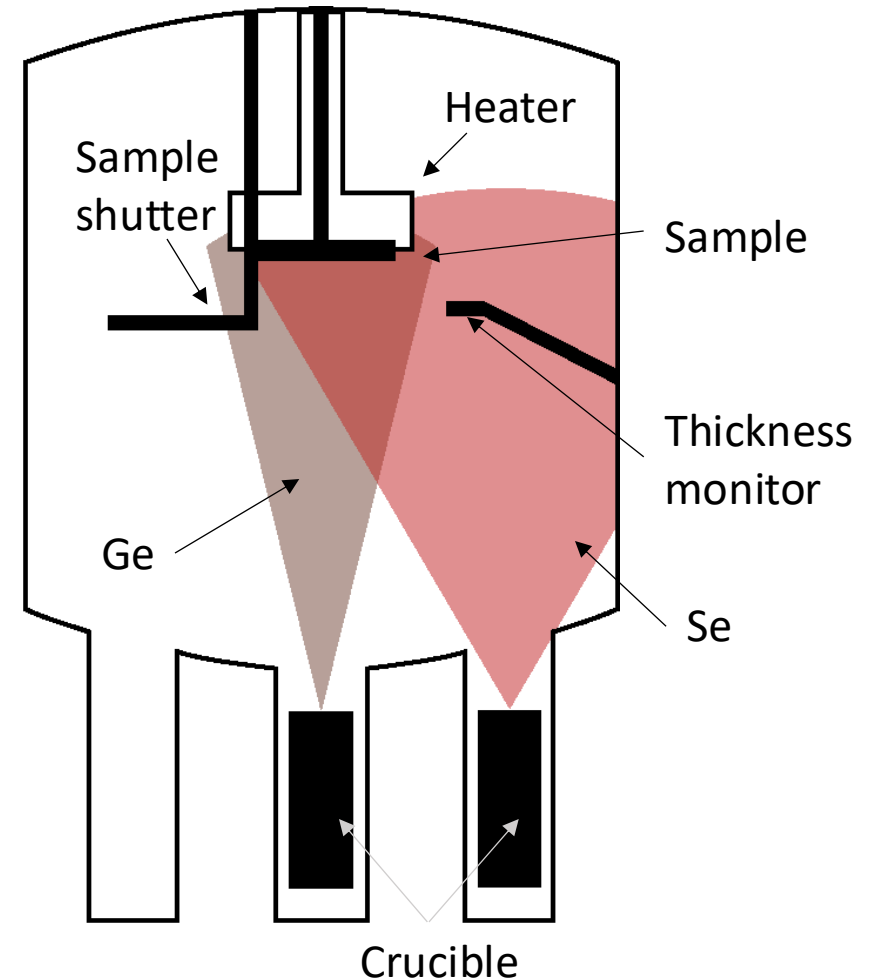


Molly McGrath
MS student



Alloying of a-Ge_xSe_{1-x}

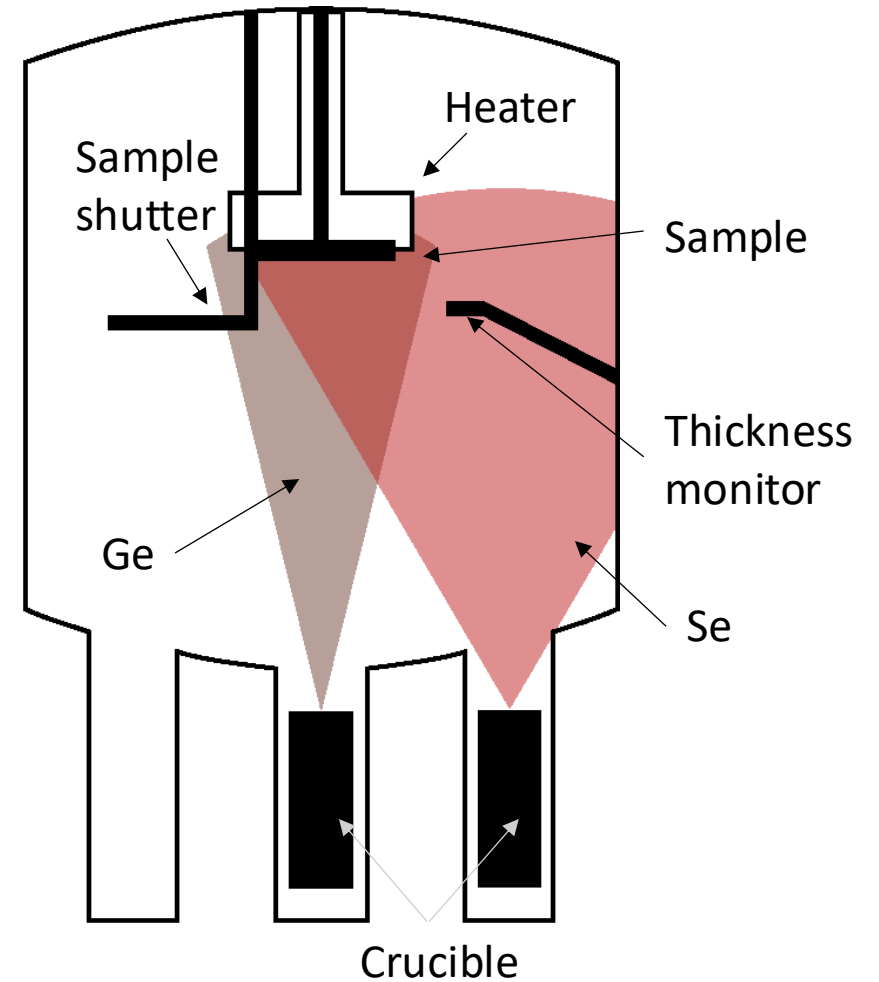
- Se melting temperature is 220 C, Ge is 938 C
 - Tested pre-alloyed pellets with Ge 10%
 - Selenium will “spit”, resulting in poor film quality and mixing
- Requires co-deposition of Se and Ge to achieve high quality, uniform films



Alloying of a-Ge_xSe_{1-x}

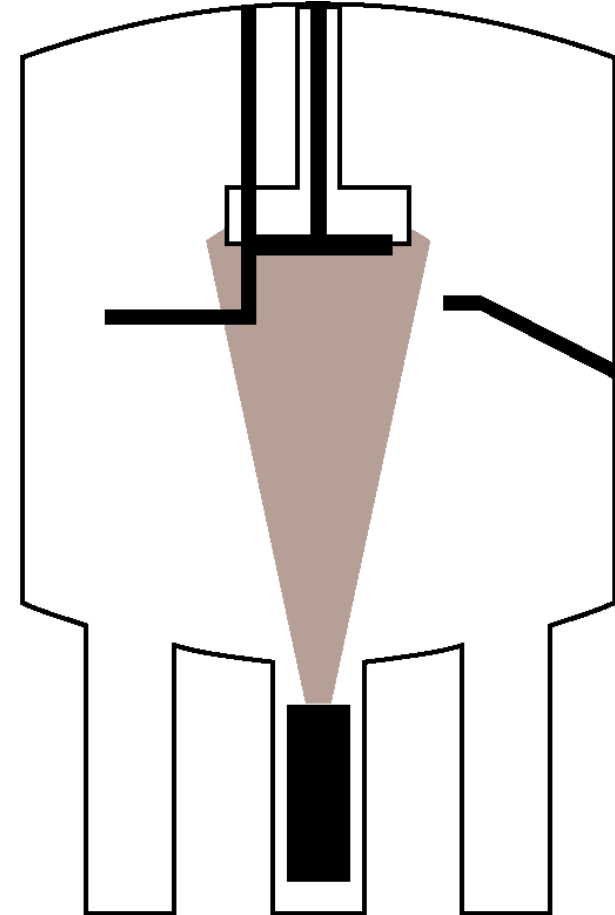
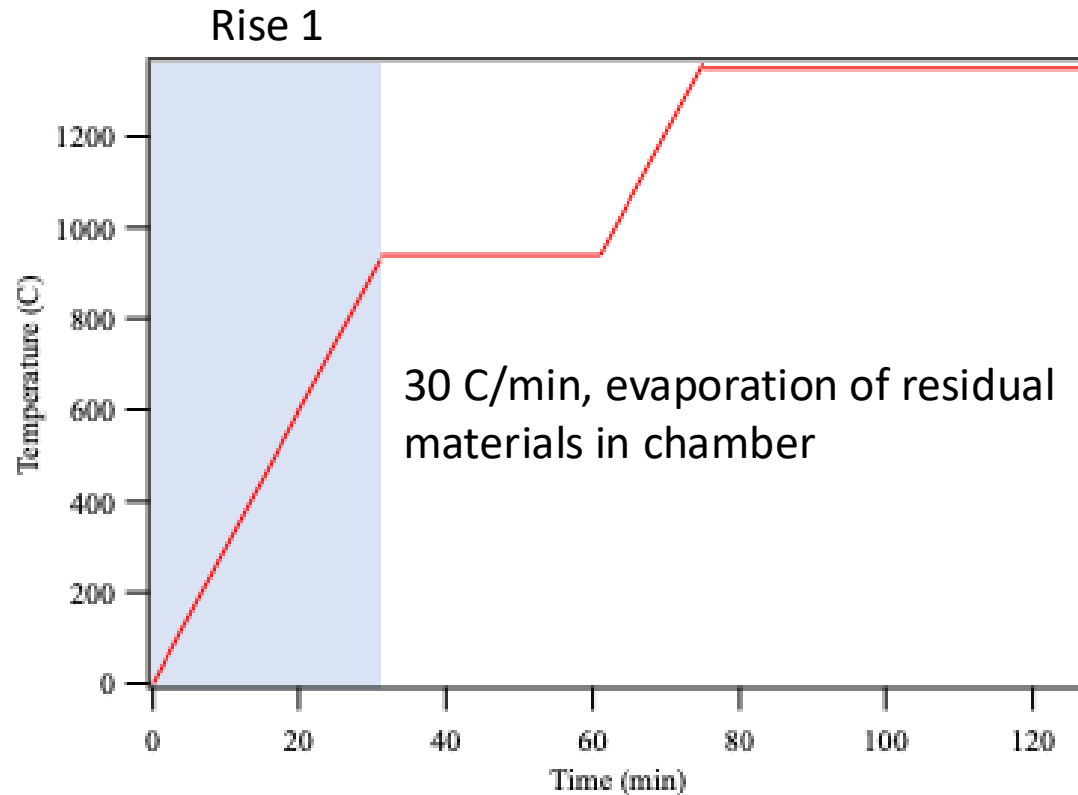
For a total thickness of 15 μm (best for ensuring full TOF measurements) we can calculate evaporation rates for each material:

Concentration n	Evaporation Rate ($\text{\AA}/\text{s}$)		Time (min)
	Ge	Se	
5%	4.0	76.0	31
7.5%	4.0	49.3	47
10%	4.0	36.0	63
12.5 %	4.0	28.0	78
15%	4.0	22.7	94
17.5%	4.0	18.9	110



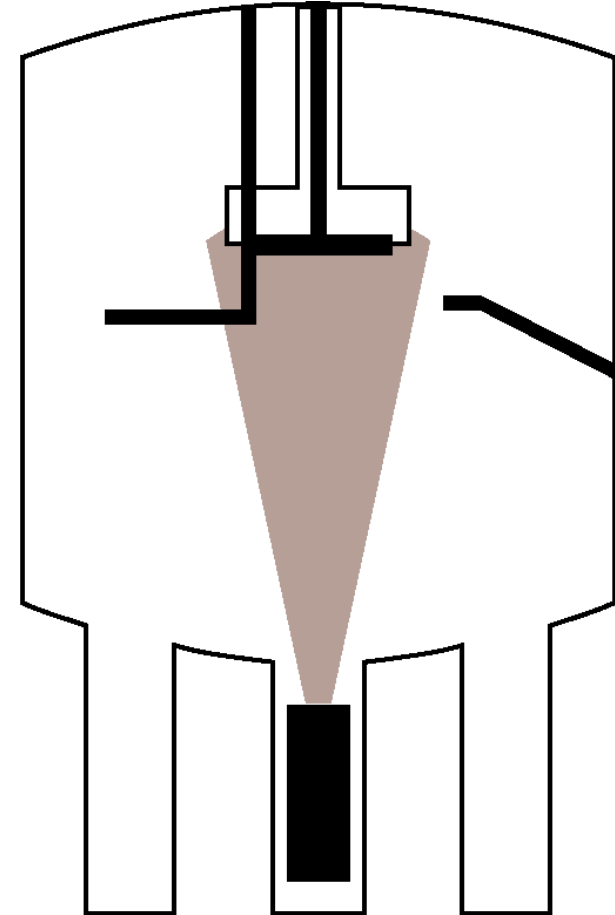
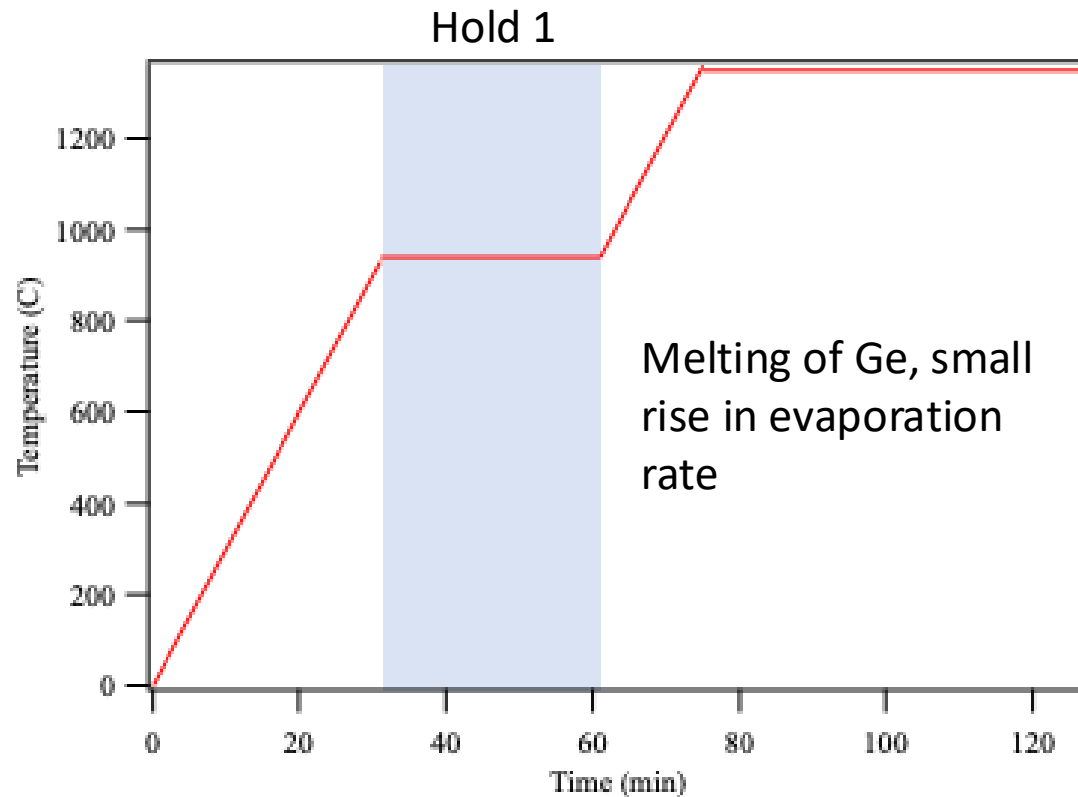
Thermal Evaporation of Ge

- While awaiting funding, we began to evaluate parameters for Ge deposition using existing system



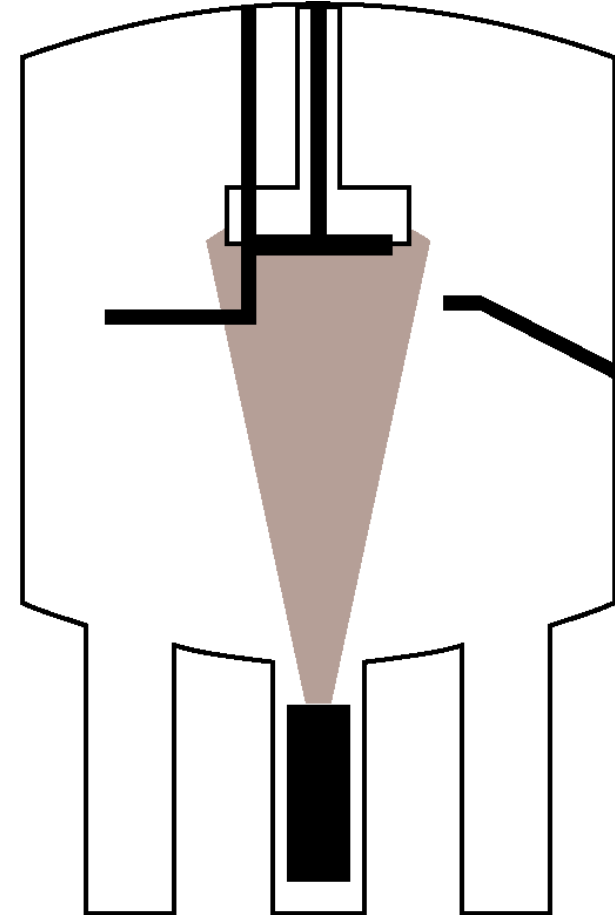
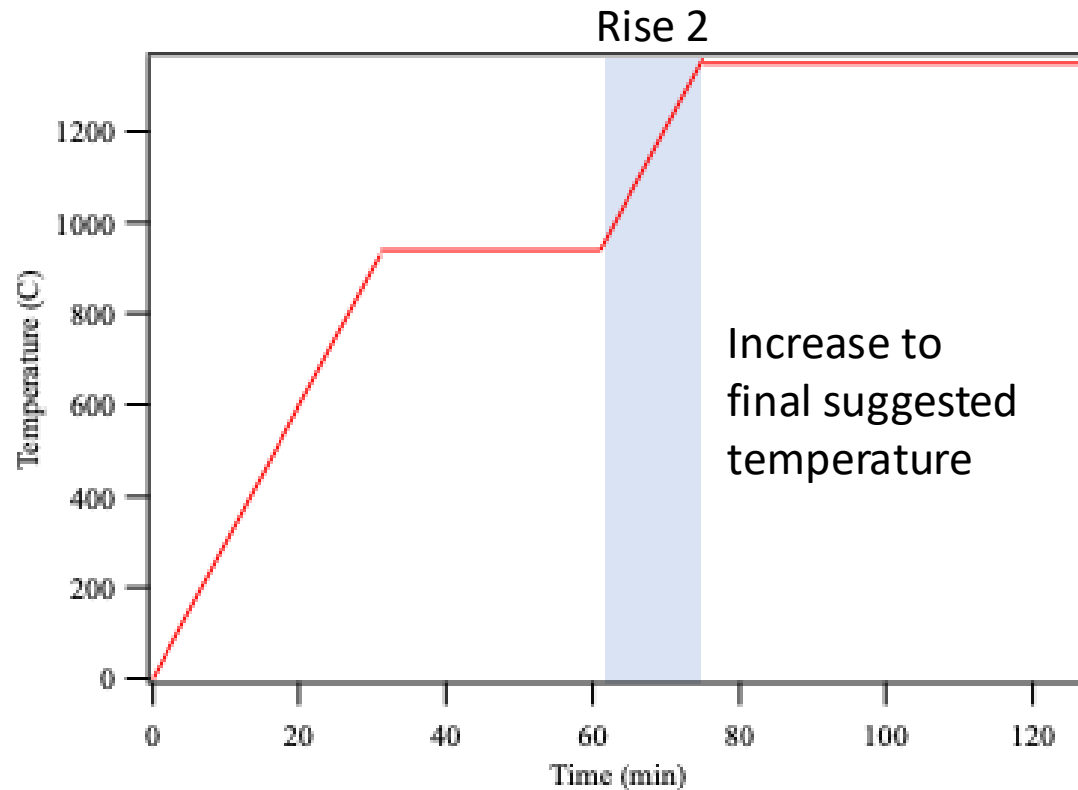
Thermal Evaporation of Ge

- While awaiting funding, we began to evaluate parameters for Ge deposition using existing system



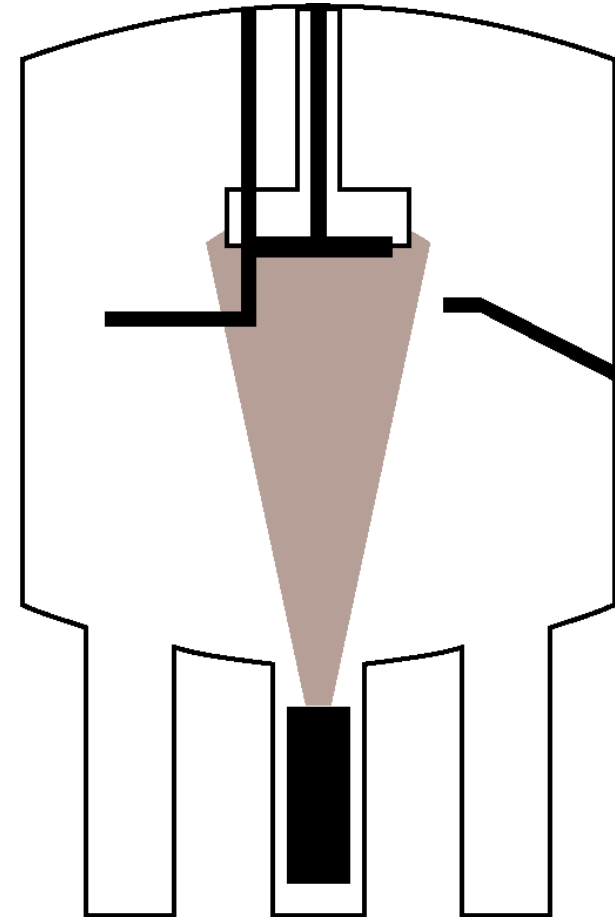
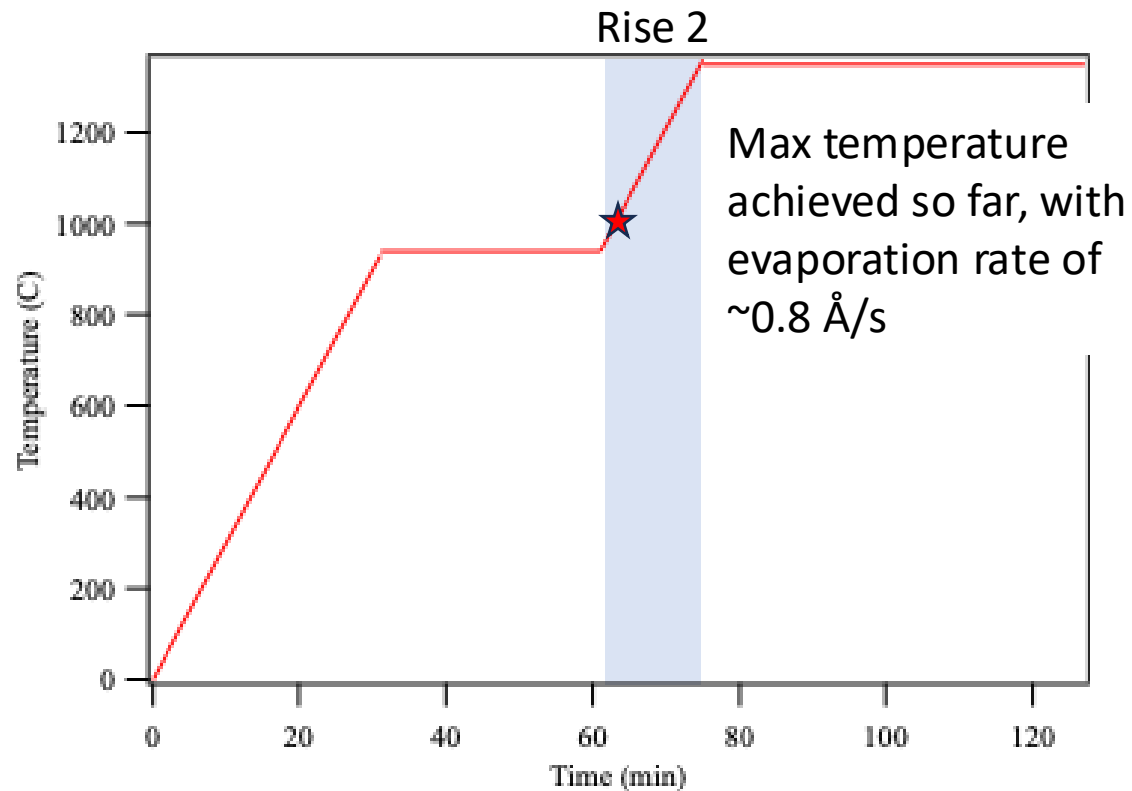
Thermal Evaporation of Ge

- While awaiting funding, we began to evaluate parameters for Ge deposition using existing system



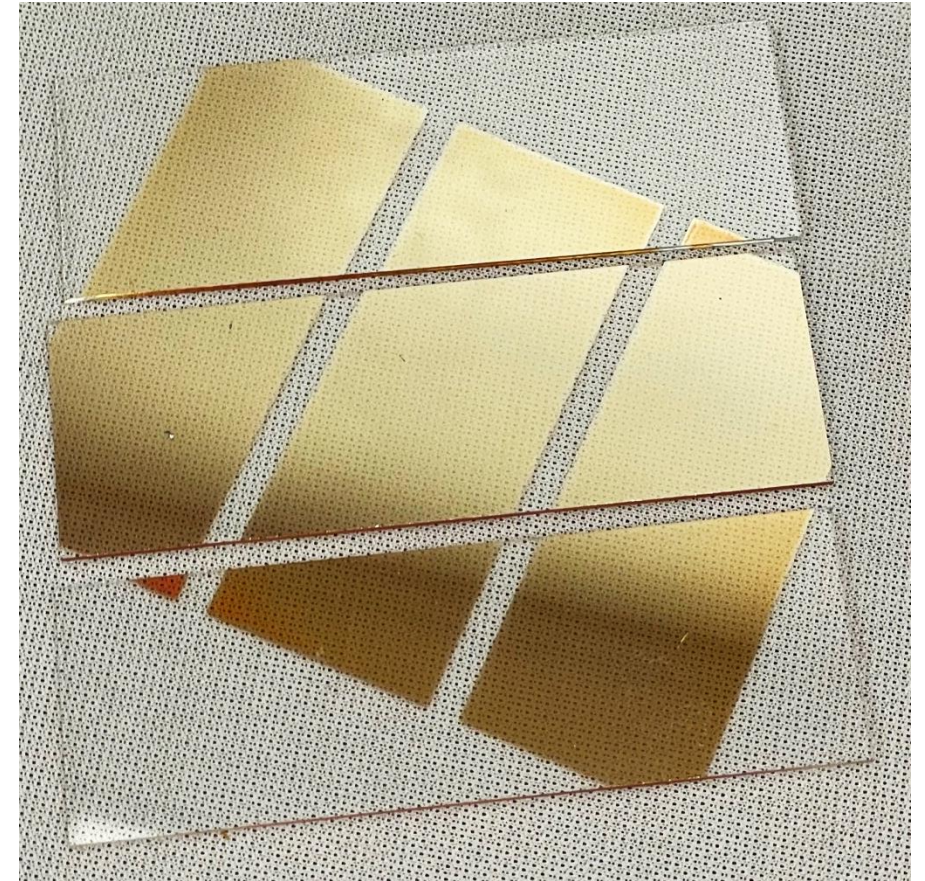
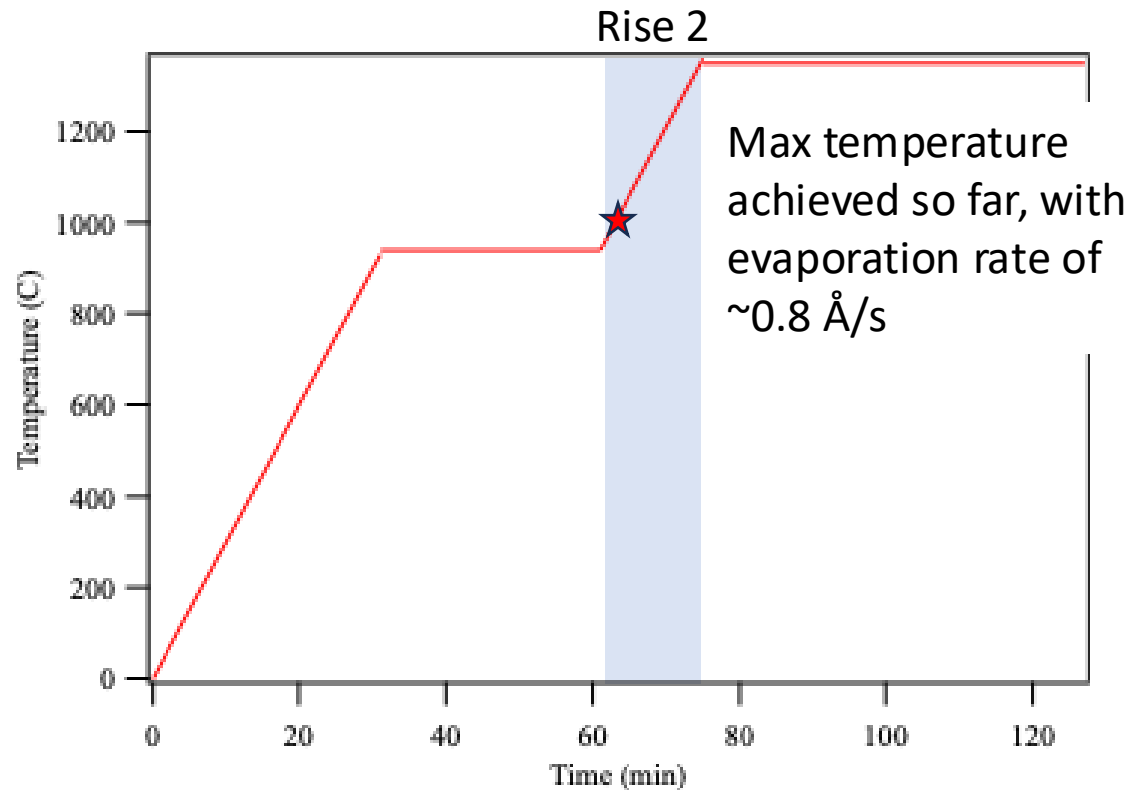
Thermal Evaporation of Ge

- While awaiting funding, we began to evaluate parameters for Ge deposition using existing system



Thermal Evaporation of Ge

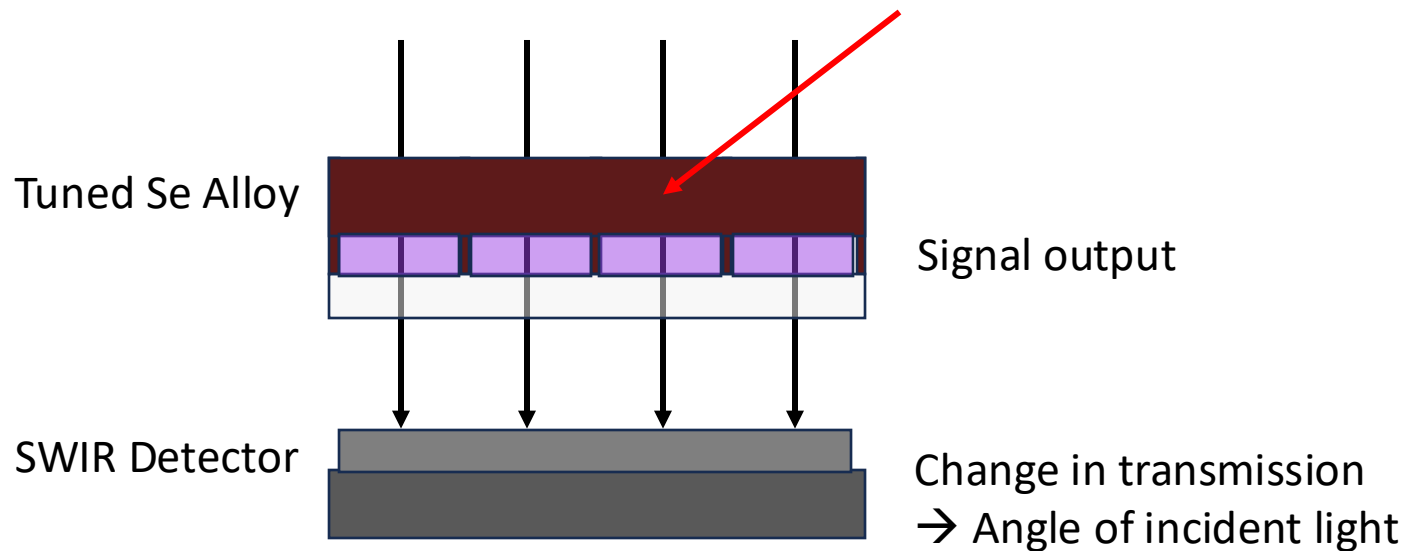
- While awaiting funding, we began to evaluate parameters for Ge deposition using existing system



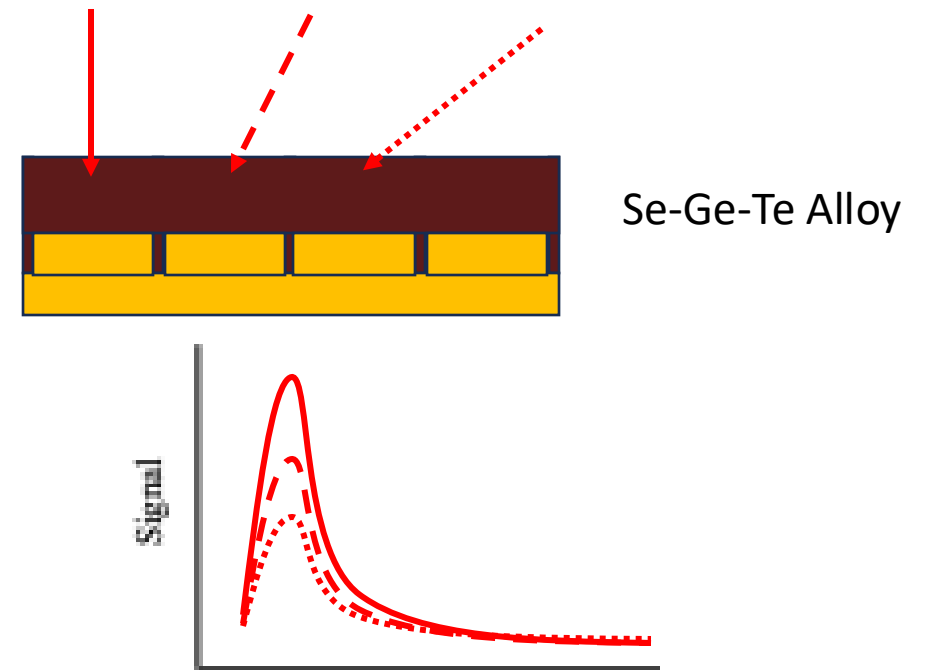
Future Applications: Photodetectors with Incident Photon Direction Sensitivity

Utilizing angle-dependence and photo-induced effects for dual-function photodetectors

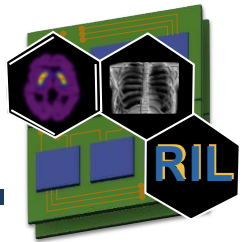
Multilayer Detector for Photon Detection and Incident Angle



Angle Dependent Signal for Low Photon Detection



Radiological Instrumentation Laboratory (RIL)



Dr. Shiva Abbaszadeh

Electrical & Computer Engineering

sabbasza@ucsc.edu

Postdoctoral Scholars

Dr. Kaitlin Hellier

Dr. Jennifer Ott (SCIPP)

Graduate Students

Gregory Romancheck (UIUC)

Akyl Swaby

Greyson Shoop

Daniel Fiallo

Kimia Gholemi

Mohammadreza Mohseni Ferezhghi

Hamid Mirzanezhad

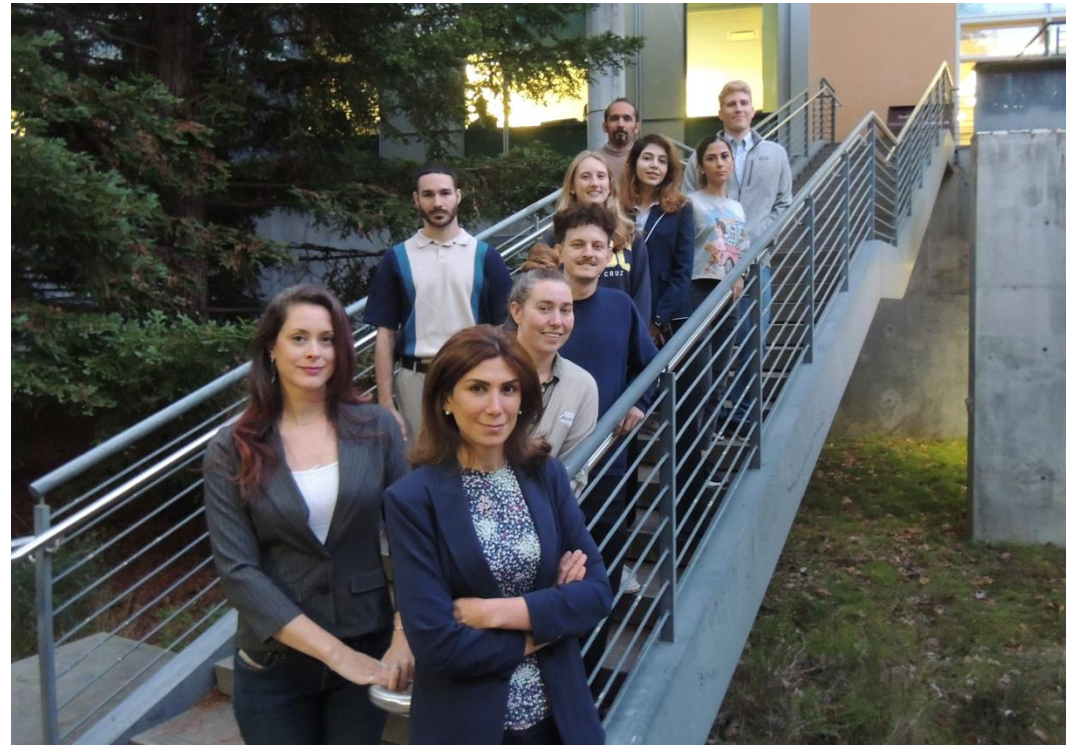
Spencer Balliet

Molly McGrath

Undergraduate Students

Max Teichera

Evelyn Cooper



Funding Provided by:

National Institute
of Health

R01EB033466



Department of
Energy High
Energy Physics

DE-SC0022343

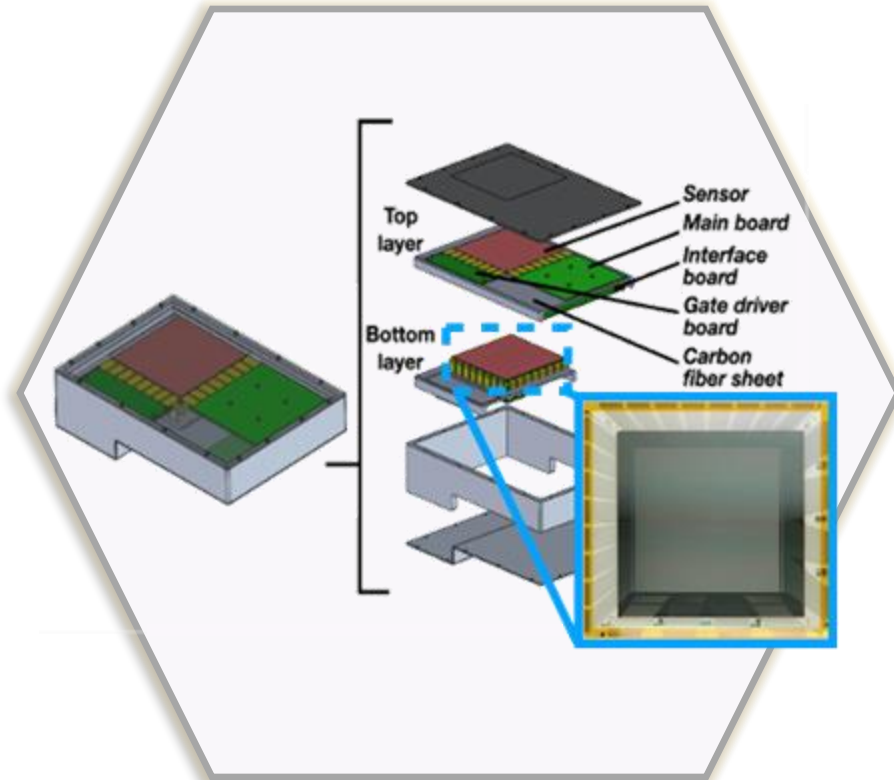


Western Digital
Corporation



Appendix

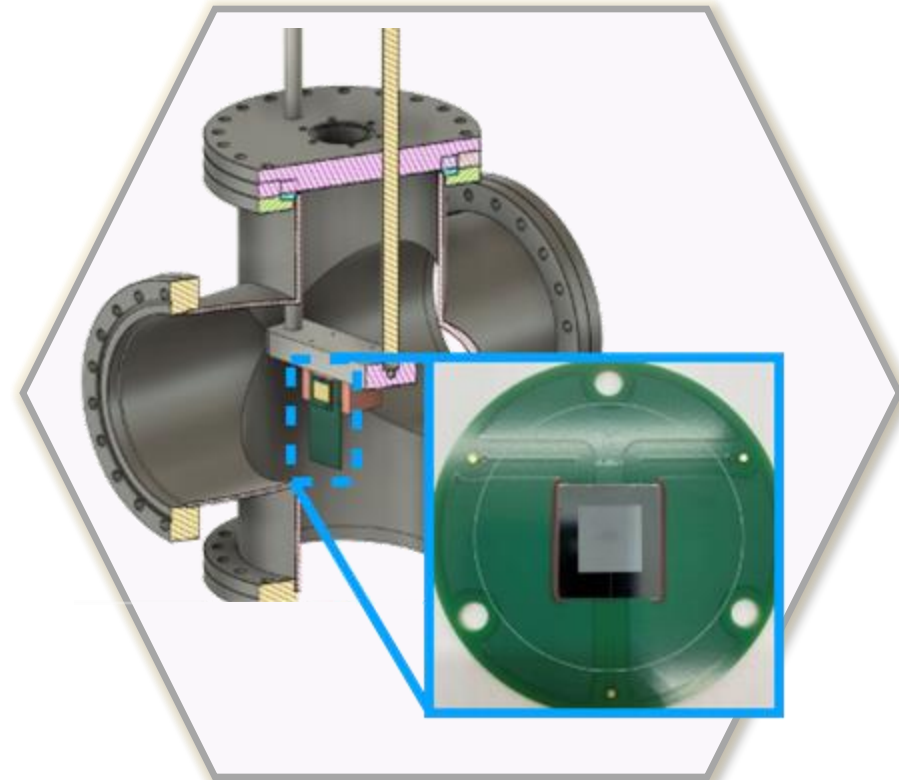
From Medical Imaging to High Energy Physics



a-Se flat panel detector

W. Zhao et al, *Medical Physics* 30, 254-263 (2003)

Hellier et al, *SPIE Medical Imaging* (2023)



Rooks, M., et al, *Journal of Instrumentation* 18, P01029 (2023).

Tzoka, I., et al., *arXiv* (2024)

Applications in direct and indirect conversion, with low-photon sensing capabilities by low-field avalanche gain

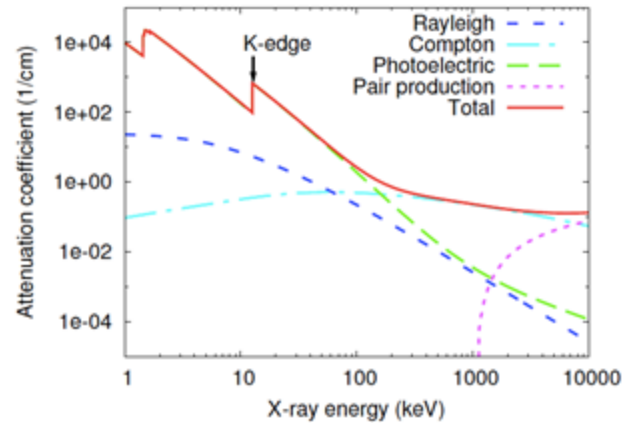
A-Se as Direct Conversion: Pushing the Limit of Spatial Resolution

Commercial panel

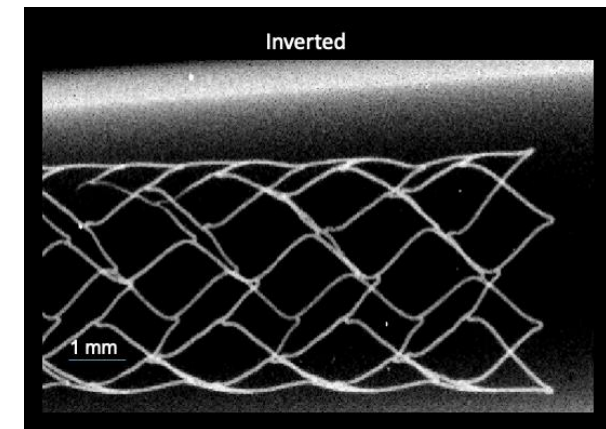


Anrad AXS-2430 a-Se
mammography panel

Attenuation properties of a-Se



Aorta stent in glass vial, 25-50 μm
wire diameter



Scott, Abbaszadeh et al., SPIE Medical Imaging, 2014.

Specifications

3T active pixel sensor

300-400e RMS noise (improvements are possible)

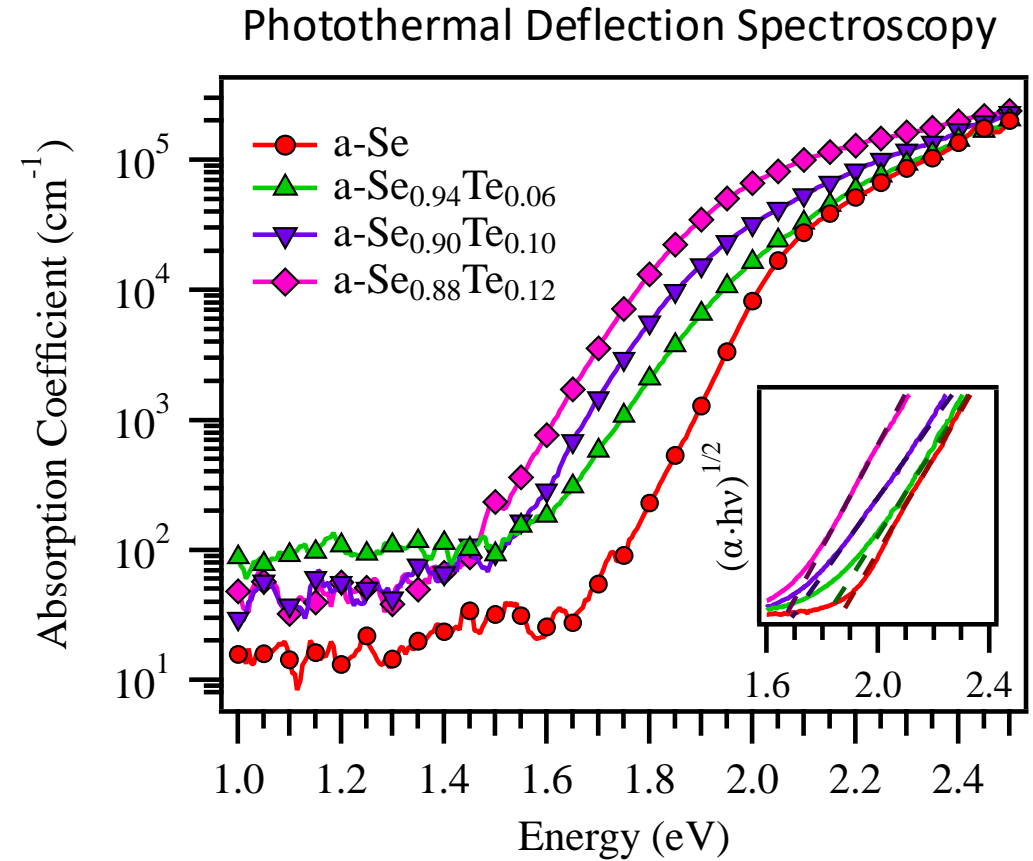
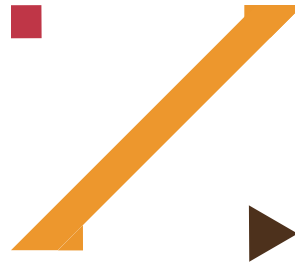
25 μm pixel pitch

640 x 640 pixel array

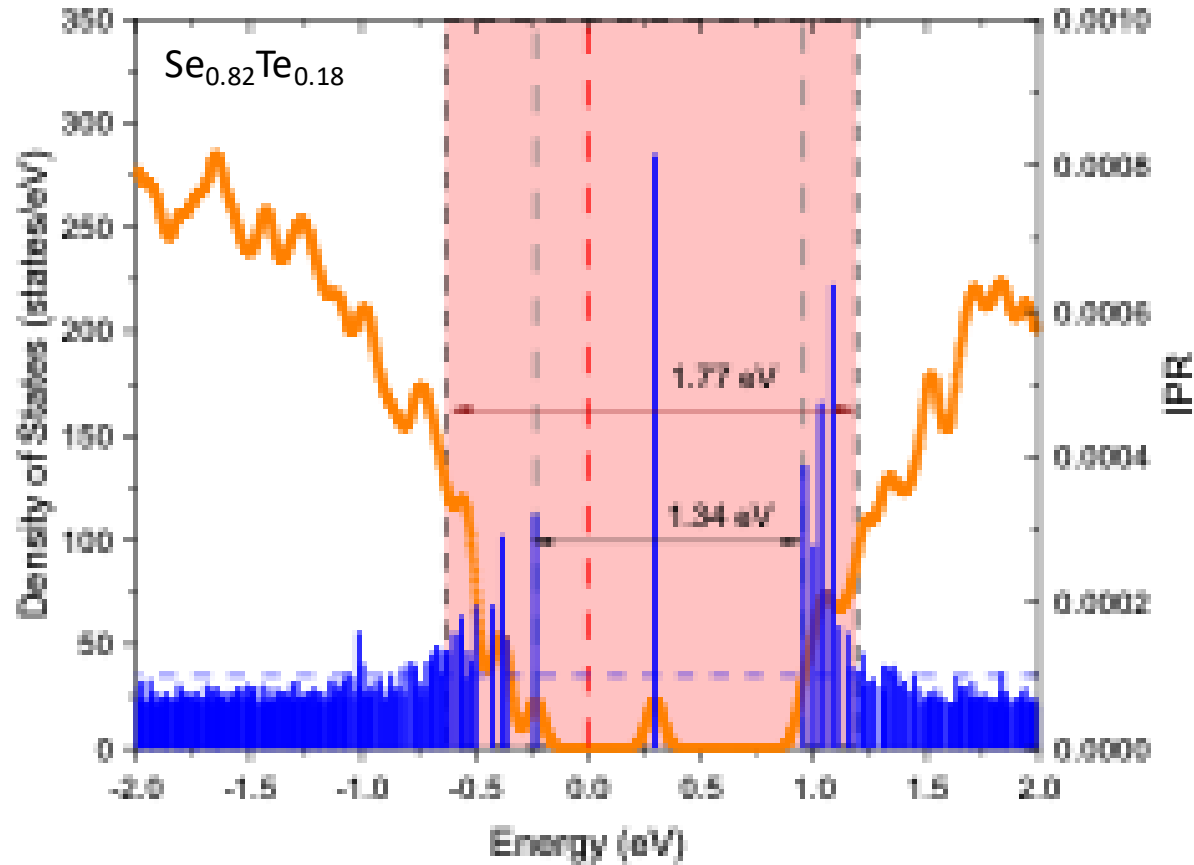
1.6 x 1.6 cm active area

Alloying of a- $\text{Se}_{1-x}\text{Te}_x$

Increasing
Te Content

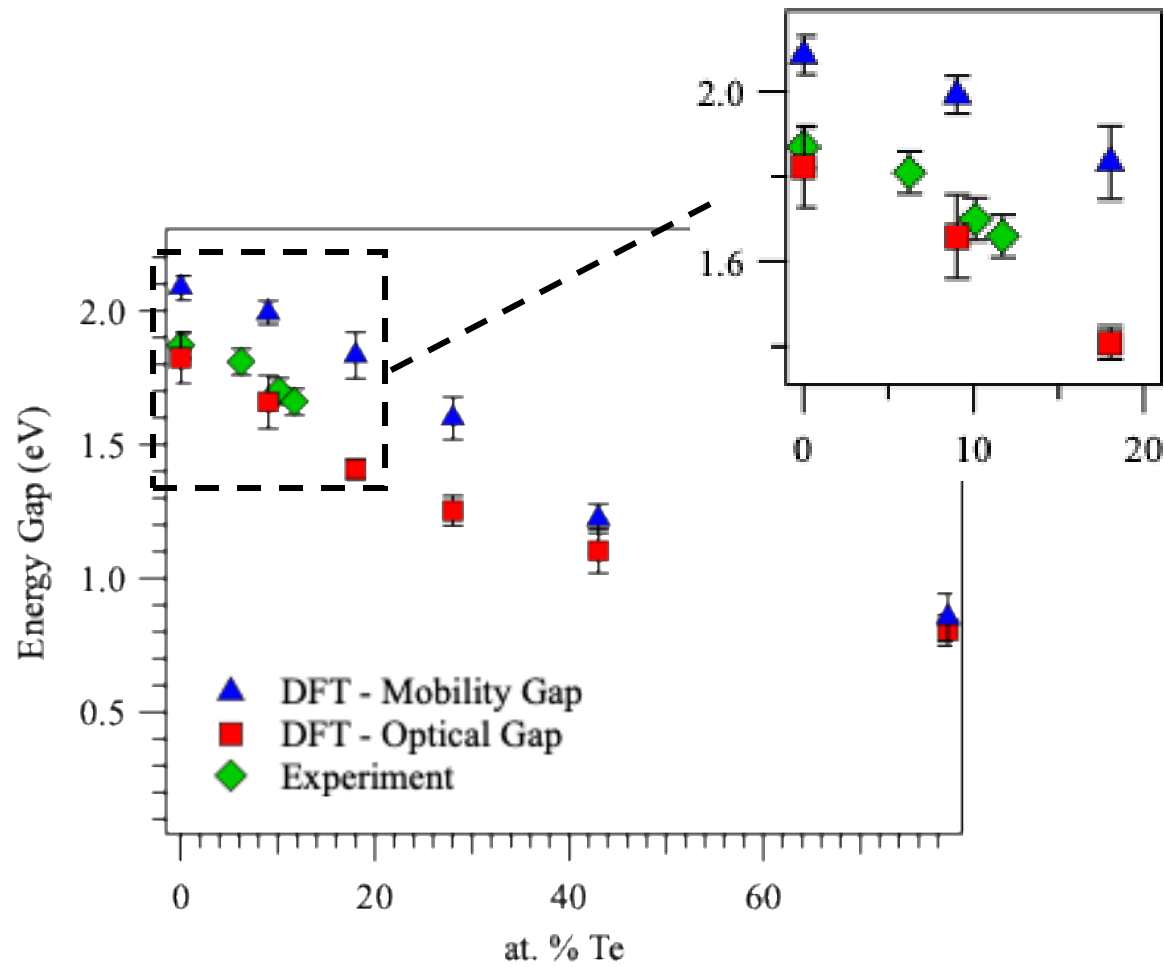


Modeling Density of States in Alloyed Se



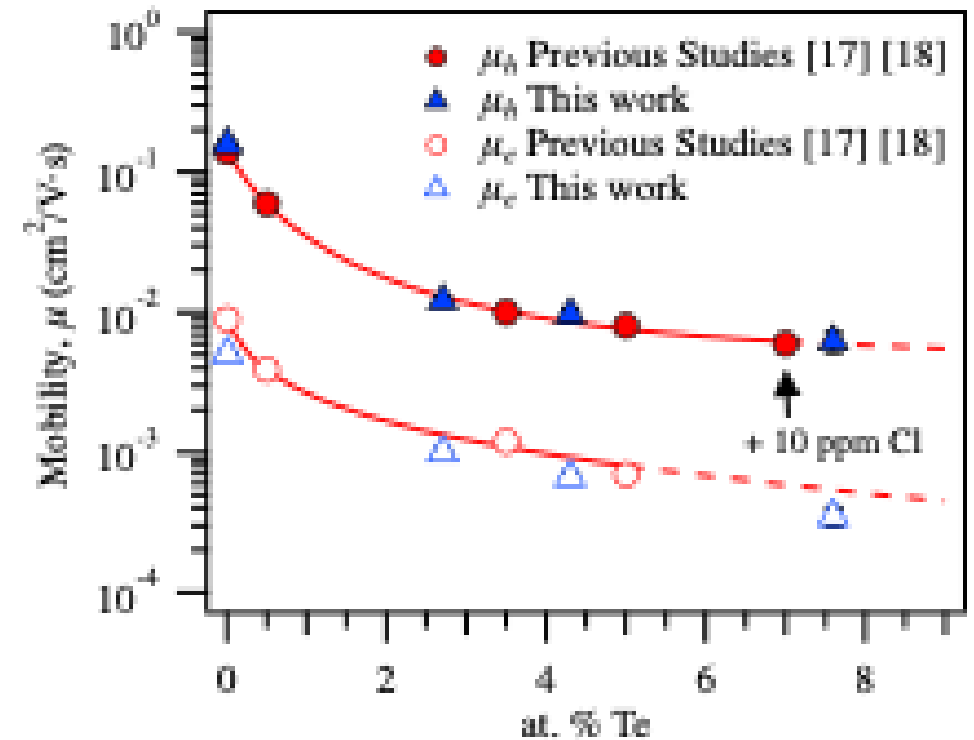
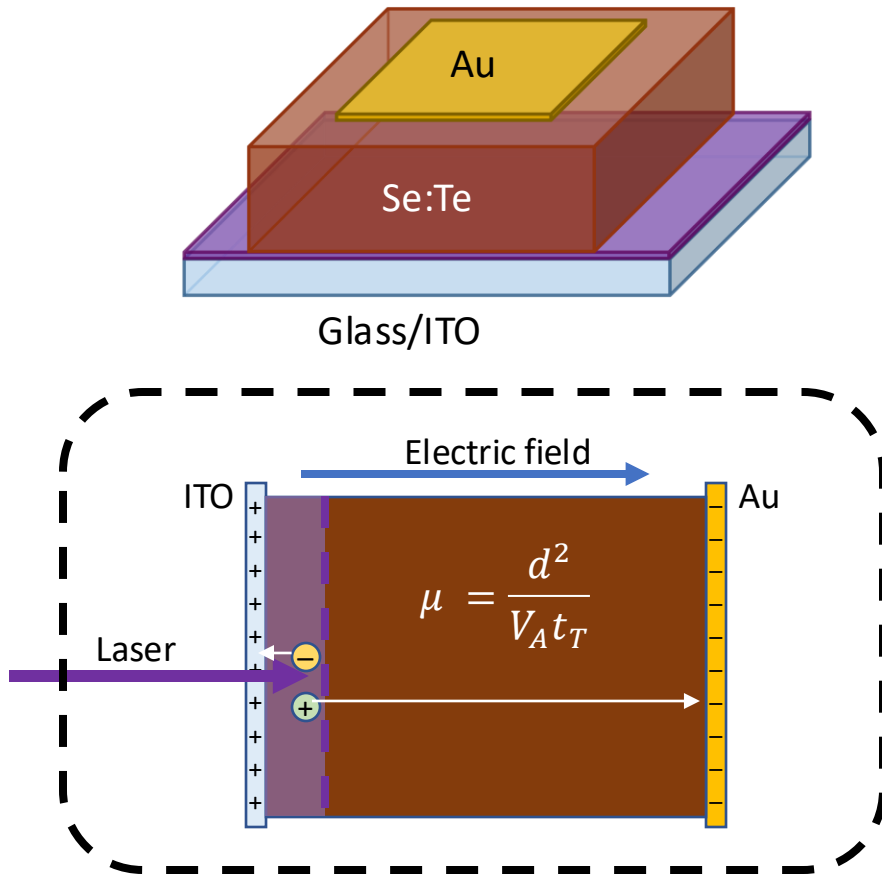
- Previous studies on Se-Te used Hybrid DFT to predict DOS
 - DOS calculated for a- $\text{Se}_{1-x}\text{Te}_x$ ($x=0, 0.9, 0.18, 0.28, 0.43, 0.79$) → Optical & Mobility Gaps
 - Inverse Participation Ratio (IPR) gives distinction between localized and delocalized states

Modeling Density of States in Alloyed Se



- Previous studies on Se-Te used Hybrid DFT to predict DOS
 - DOS calculated for a- $\text{Se}_{1-x}\text{Te}_x$ ($x=0, 0.9, 0.18, 0.28, 0.43, 0.79$) \rightarrow Optical & Mobility Gaps
 - Inverse Participation Ratio (IPR) gives distinction between localized and delocalized states
- Predicted optical gaps in-line with those found in experiment
- Se-Te known to crystallize for $\text{Te} > 30\%$ \rightarrow reduced separation of mobility and optical gap
- **Hybrid DFT allows for reasonable prediction of optical and electronic states in new materials \rightarrow Ge-Se**

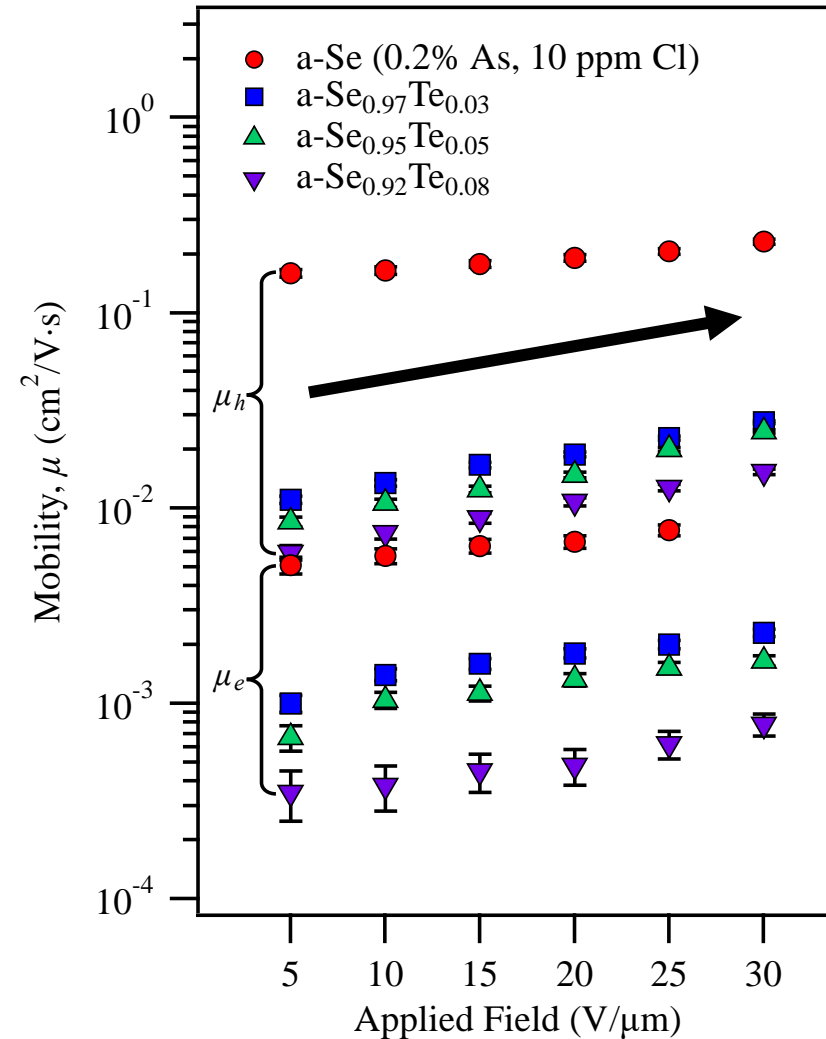
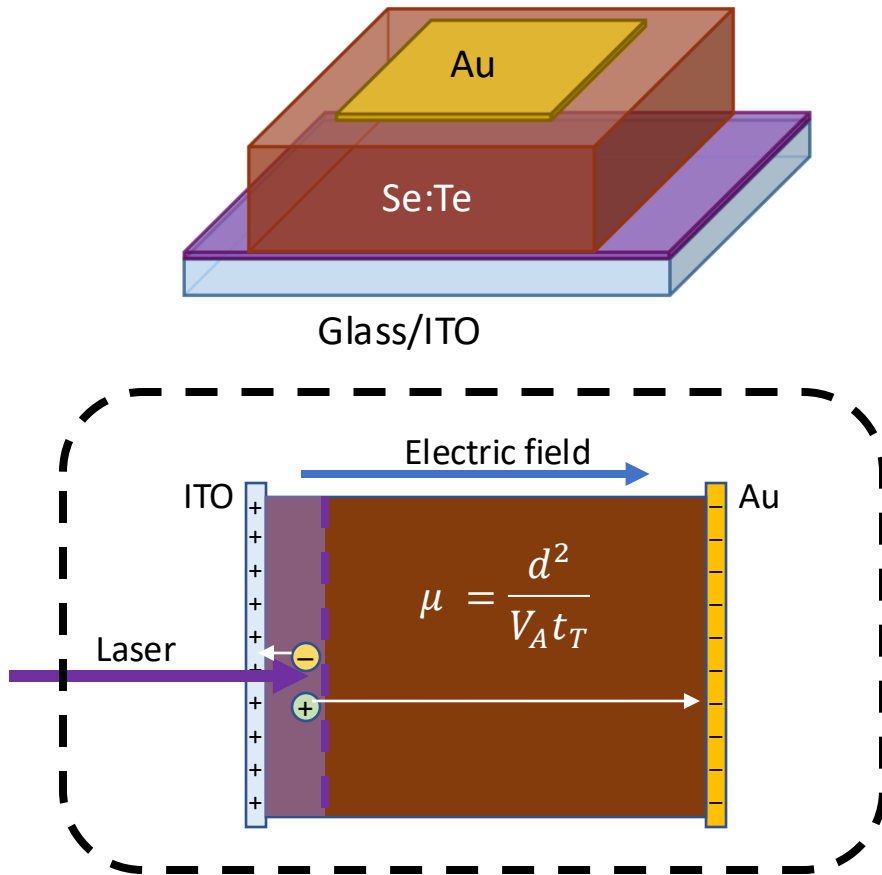
Alloying of a- $\text{Se}_{1-x}\text{Te}_x$



[17] Kasap and Juhasz, *J. Non-Cryst. Sol.* (1985), v 72, 1, p 23

[18] Juhasz et al., *J. Mat. Sci.* (1987), v 22, 7, p 2569

Alloying of a-Se_{1-x}Te_x

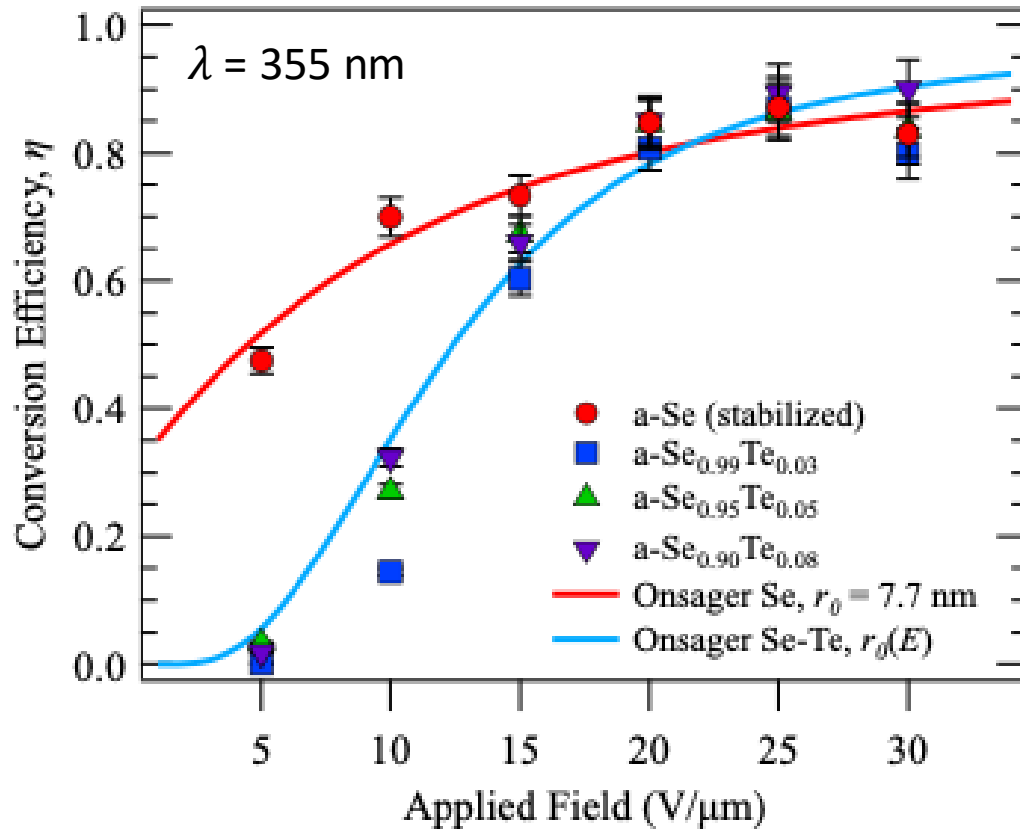


Hellier et. al, *ACS AEM* (2023), v 5, 5, p 2678

Kasap and Juhasz, *J.Non-Cryst. Sol.* (1985), v 72, 1, p 23

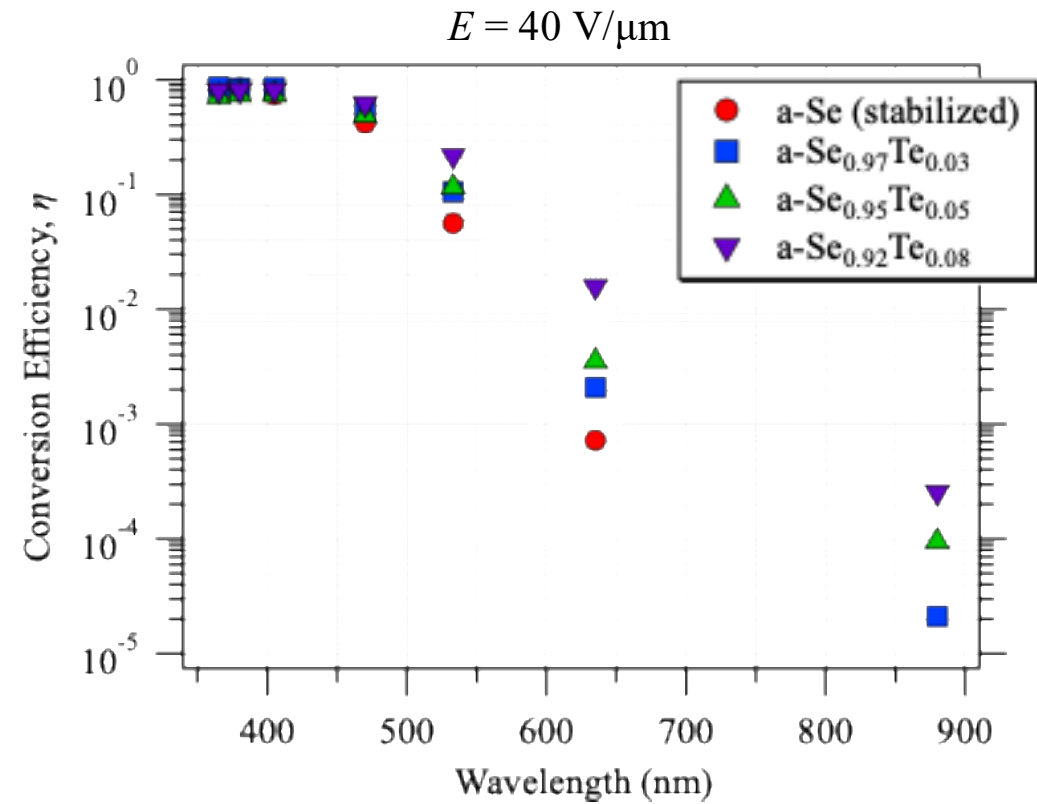
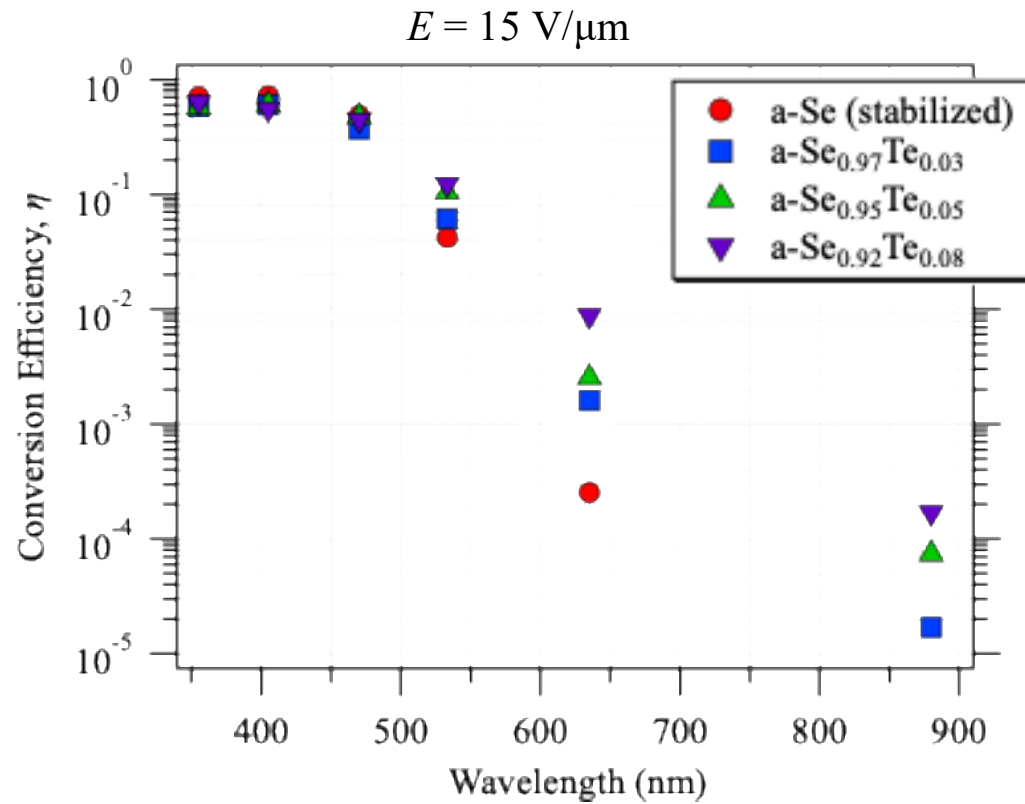
Juhasz et a., *J. Mat. Sci.* (1987), v 22, 7, p 2569

Alloying of a- $\text{Se}_{1-x}\text{Te}_x$



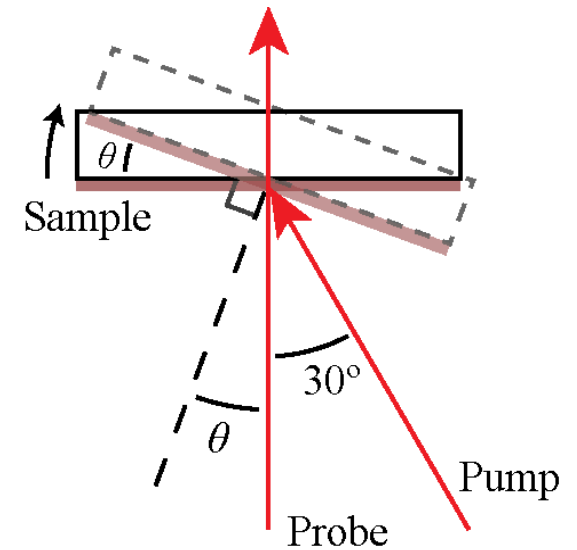
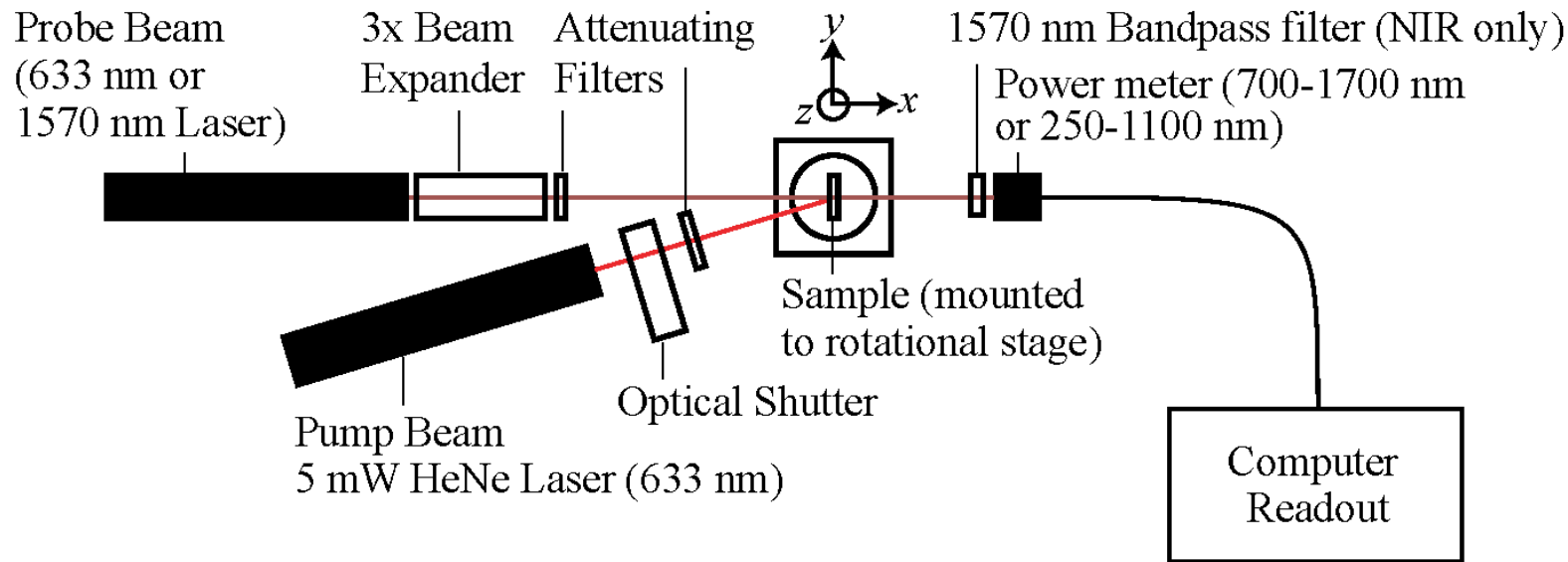
- At low fields, CE limited by trap states and low thermalization
 - At moderate to high fields, CE recovers as carriers gain enough energy to escape traps
- Modified Onsager model, with thermalization length (r_0) a function of field – not just wavelength

Alloying of a- $\text{Se}_{1-x}\text{Te}_x$

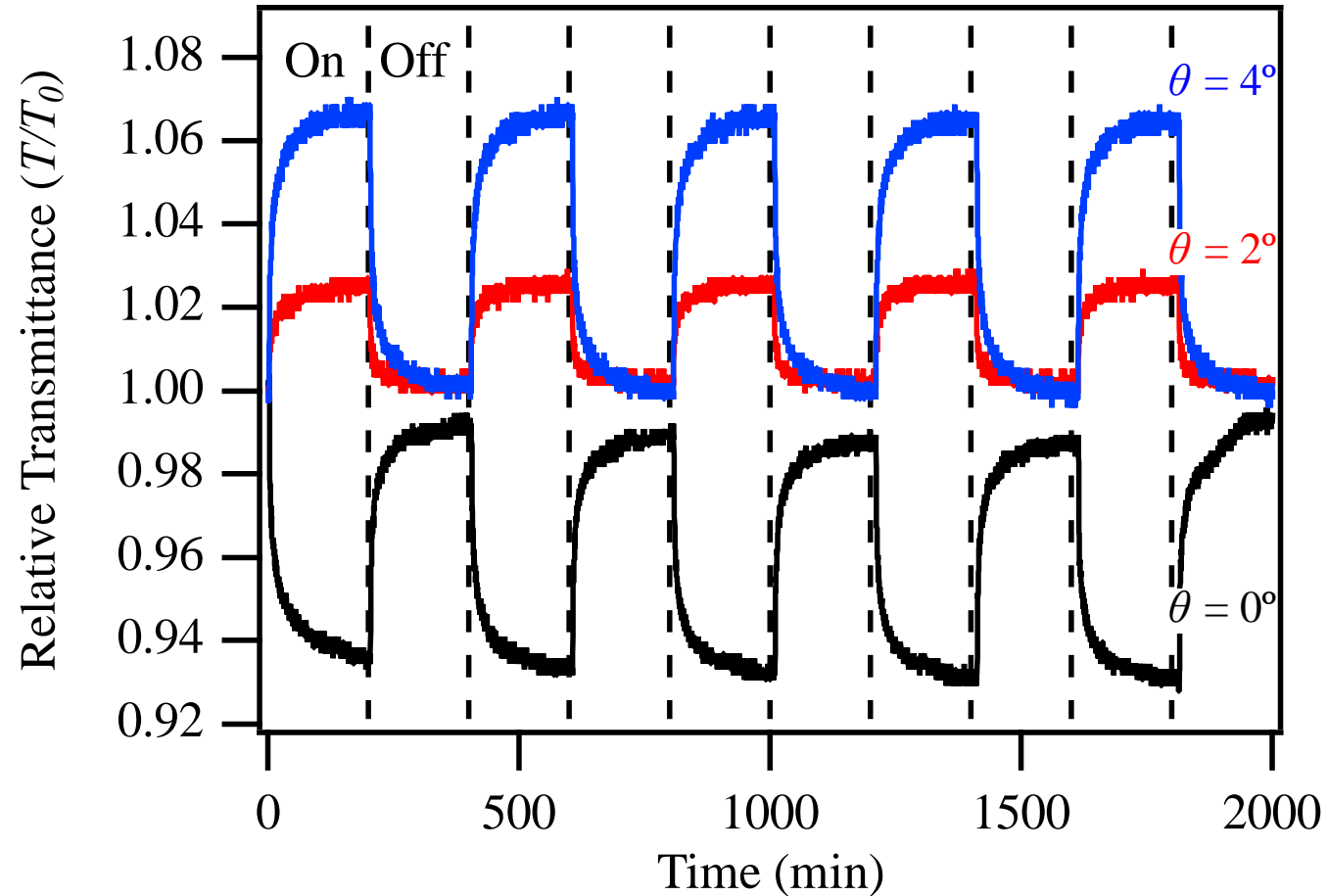


Increasing Te concentration \rightarrow increased CE at long wavelengths, especially at higher fields

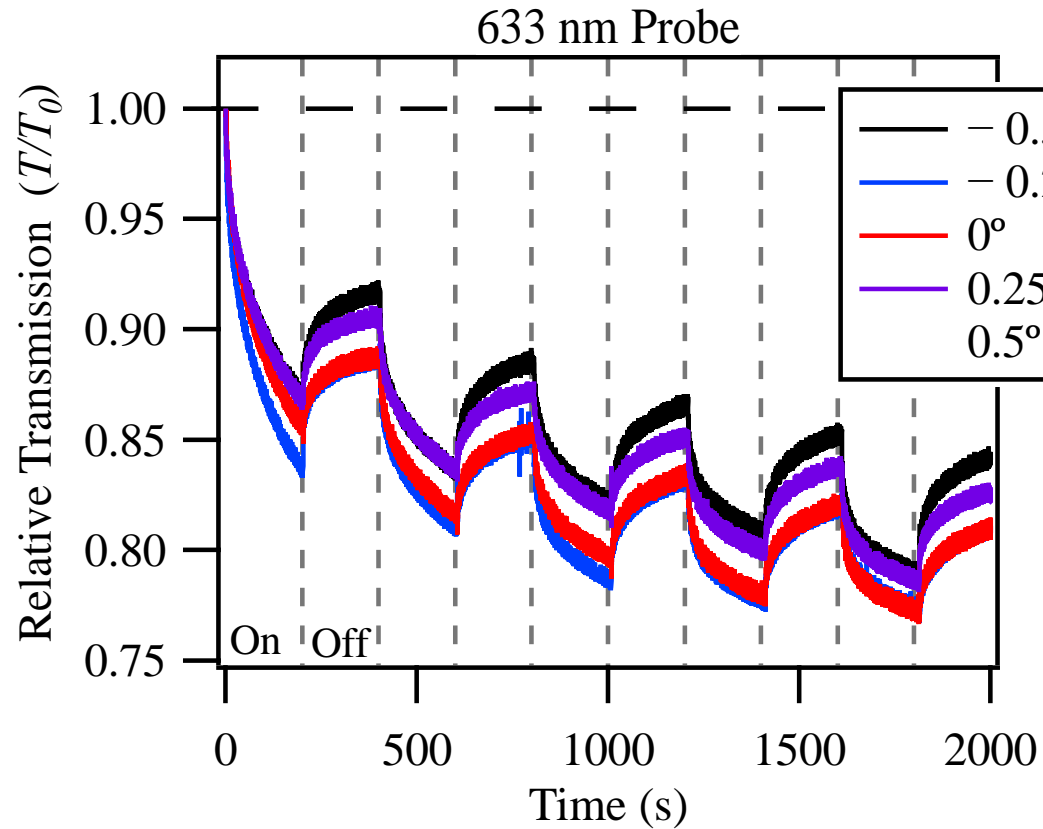
Testing effects of angle on photodarkening behavior



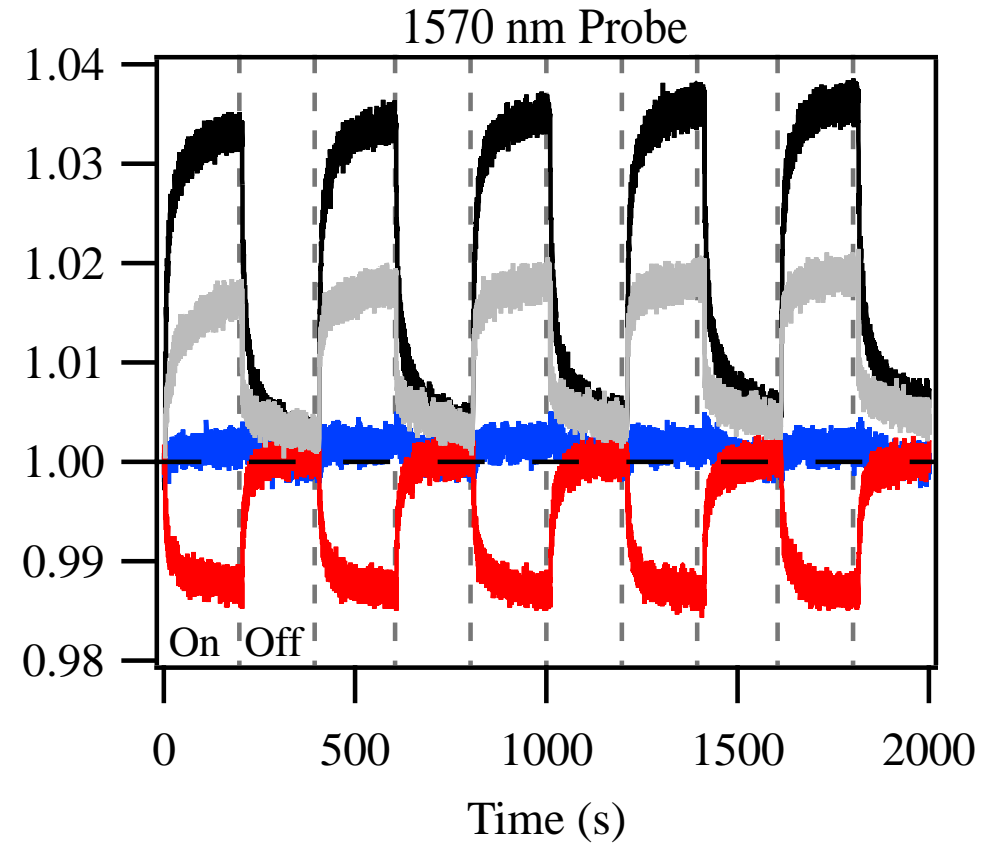
Effects of angle on photodarkening behavior



Effects of angle on photodarkening behavior



(a)



(b)

Effects of angle on photodarkening behavior

